



Cite this: *RSC Adv.*, 2022, 12, 7689

Received 16th October 2021  
Accepted 22nd February 2022

DOI: 10.1039/d1ra07657d

rsc.li/rsc-advances

# Tannic acid: a crosslinker leading to versatile functional polymeric networks: a review

Chen Chen, <sup>b</sup> Hao Yang, <sup>a</sup> Xiao Yang <sup>\*a</sup> and Qinghai Ma <sup>\*a</sup>

With the thriving of mussel-inspired polyphenol chemistry as well as the demand for low-cost analogues to polydopamine in adhesive design, tannic acid has gradually become a research focus because of its wide availability, health benefits and special chemical properties. As a natural building block, tannic acid could be used as a crosslinker either supramolecularly or chemically, ensuring versatile functional polymeric networks for various applications. Up to now, a systematic summary on tannic-acid-based networks has still been waiting for an update and outlook. In this review, the common features of tannic acid are summarized in detail, followed by the introduction of covalent and non-covalent crosslinking methods leading to various tannic-acid-based materials. Moreover, recent progress in the application of tannic acid composites is also summarized, including bone regeneration, skin adhesives, wound dressings, drug loading and photothermal conversion. Above all, we also provide further prospects concerning tannic-acid-crosslinked materials.

## 1. Introduction

Natural-resource-rich building blocks that can polymerize into functional composites have long been a source of scientific inspiration.<sup>1,2</sup> When it comes to complex superstructures, obtained from the assembly of simple naturally derived building blocks, they have gained widespread interest for engineering materials with improved and synergistic properties.<sup>3,4</sup> With the aim of meeting complex biological requirements, the charm of natural materials lies in the exploitation of organic and inorganic building blocks to prepare hybrid materials with synergistic properties.<sup>5</sup> Plant polyphenols, classified as a family of naturally derived compounds, contain a high concentration of dihydroxyphenyl (catechol) or trihydroxyphenyl (pyrogallol) moieties that link to versatile biological functions such as corrosion resistance, coloration, mechanical reinforcement, and prevention of radiation damage.<sup>6,7</sup> A person who has a high dietary intake of polyphenols generally has a lower incidence of tumor diseases, osteoporosis, and diabetes as well as neurodegenerative and cardiovascular diseases.<sup>8</sup> The rising interest in polyphenols over the past few decades is attributable to their broad spectrum of molecular tectonics and chemical properties.<sup>9</sup>

Tannic acid (TA) is a natural polyphenol, which exists in a wide variety of plants as a colourless to pale yellow solid with an astringent taste (Fig. 1). TA could be exacted from natural

sources such as the bark of oak, chestnut, hemlock, and mangrove and the leaves of certain sumacs and plant galls.<sup>10</sup> With multiple ways of obtaining it, TA is the most abundant natural compound after cellulose, hemicellulose and lignin, serving as a crucial commercial raw material and has traditionally been utilized as a tanning agent in leather, coating, adhesive, surgery, pharmaceutical and food industrial applications.<sup>11</sup> Since tannic acid contains a complex compound of

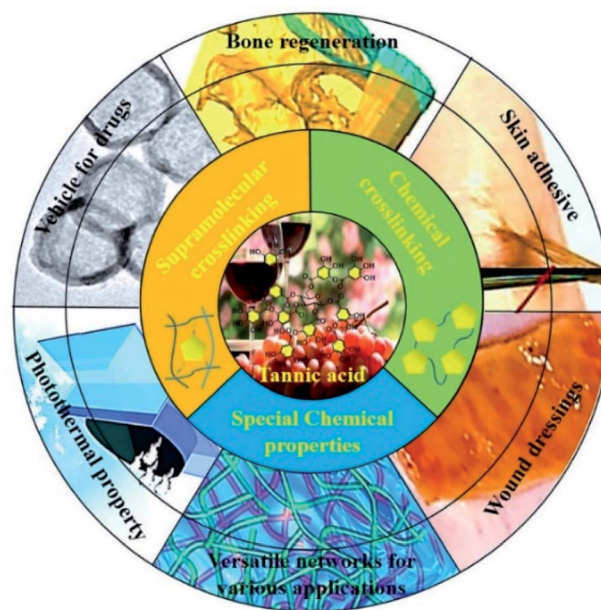


Fig. 1 Versatile networks derived from tannic acid and their wide scope of applications.

<sup>a</sup>The First Affiliated Hospital of Shandong First Medical University (Shandong Qianfoshan Hospital), Jinan 250014, China. E-mail: 2485@sdhospital.com.cn; maqinghai@sdhospital.com.cn

<sup>b</sup>Key Laboratory of New Material Research Institute, Department of Acupuncture-Moxibustion and Tuina, Shandong University of Traditional Chinese Medicine, Jinan 250355, China



polyphenols, which contain numerous catechol and pyrogallol aromatic ring structures, a series of unique chemical properties can be listed. (i) The water solubility of TA: TA has a solubility of  $300 \text{ g L}^{-1}$  in water, which is suitable for chemical modification in a green way. Moreover, the TA aqueous solution is stable in air and can be stored in the lab for more than 30 days.<sup>12,13</sup> (ii) The biocompatibility of TA: TA is a natural polyphenol that is cheap in price, environmentally harmless, widely available, and generally biocompatible.<sup>14</sup> Furthermore, TA is hydrolysable as well as biodegradable under certain hydrolytic conditions, in which the breakage of the ester linkage between two pyrogallol groups plays a significant role.<sup>15</sup> (iii) Universal adhesiveness of TA: the various intermolecular reactions between TA and various nucleophiles (amide bonds, thiols and amines) on a protein-rich tissue surface endow a TA-derived material with superior skin affinity and underwater adhesion capacity.<sup>16</sup> (iv) The metal-chelating properties of TA: TA can participate in biological processes through significant functional metal chelation, which emerged as a facile method for constructing new frameworks and sensors.<sup>17,18</sup> Moreover, with a bunch of *o*-dihydroxy and trihydroxy aromatic rings, this naturally extracted compound can reduce noble metal ions (*e.g.*,  $\text{Au}^{\text{III}}$  and  $\text{Ag}^{\text{I}}$ ) to corresponding metallic nanoparticles (NPs).<sup>19</sup> At this point, TA plays a role as a large molecular stabilizer to provide stabilization to the NPs formed from the chelated metal species because of the steric hindrance provided by aromatic rings, and the electron donation/acceptance interactions among adjacent phenolic groups.<sup>20</sup> (v) Supramolecular conjugation between TA and polymers: researchers have proved that TA has the ability to interact with biomacromolecules such as chitosan, collagen, gelatin, silk fiber, and albumin *via* supramolecular interactions.<sup>21</sup> For instance, TA has high hemostatic efficiency since it could conjugate with various proteins in blood, leading to instant coagulation.<sup>22</sup> Characteristically, abundant hydrophobic phenyl groups enable TA to adsorb firmly to a graphene nano-sheet *via*  $\pi$ - $\pi$  stacking, endowing graphene with water dispersion stability since a large number of hydrophilic phenolic hydroxyl groups decorate the graphene surface.<sup>23</sup> The benzene rings of TA can also trigger  $\pi$ - $\pi$  conjugation with the benzene ring of dye molecules.<sup>24</sup> (vi) Clinical uses of TA: TA is also recognized as an anti-bacterial, anti-oxidant, anti-viral and anti-inflammation agent,<sup>25</sup> and has been applied as a precise therapy for burn wounds and other therapeutic applications.<sup>26,27</sup> (vii) UV-adsorption property of TA: As a widely distributed polyphenol in plant cells and tissues, TA possess broad absorption across UV regions, which is promising in skin protection.<sup>28</sup>

Because of its specific polyhydric phenol structure, TA was found to be able to function as a crosslinker either physically or chemically, resulting in the emergence of versatile polymeric networks. When it comes to physical or supramolecular crosslinking, TA is able to complex or crosslink macromolecules at multiple binding sites through multiple interactions, including hydrogen bonding, ionic bonding and  $\pi$ - $\pi$ /cation- $\pi$  interactions.<sup>29</sup> Three illustrative examples on these interactions in daily life are given here: (1) researchers found that TA present in red wine or tea accounts for the deposition of a coating on the inner surface of the containers in which those liquids are stored.<sup>30</sup> In

daily life, pyrogallol-rich liquids such as red wine, red tea, and coffee were also capable of successfully coating TA on flexible surfaces *via* intermolecular hydrogen bonds.<sup>31</sup> (2) With reference to textile dyeing and coloration processes, TA can induce mordant combinations on a textile surface *via* the formation of a metal-phenolic network, manifesting that TA has desirable metal ion chelating/reducing capability.<sup>32</sup> (3) Specifically, TA-based decoration of graphene or nanocarbon tubes has been proved to be a cost-effective and environmentally-friendly strategy leading to hybrid functional composites.<sup>33</sup> Not confined to physical crosslinking to construct supramolecular materials, TA can also react with other functional molecules to form a covalent polymeric network *via* chemical crosslinking. Therefore, versatile functional polymers can be derived from TA-based polyphenol chemistry, which are promising in fields such as adhesive hydrogels, drug loading nano-carriers, thermosets, tissue engineering and so on (Table 1).

## 2. Physical/supramolecular crosslinking

Programmed crosslinking of functional molecules into 3D networks in non-covalent ways is a general route to obtain supramolecular materials, requiring the involvement of polymers or monomers to provide functional groups allowing the formation of dynamic supramolecular interactions through physical crosslinking. Nonetheless, some desirable functional groups in general do not exist in most water-soluble polymers.<sup>34</sup> A tedious post-functionalization method through covalent bonding of the useful moieties onto polymer chains is normally used to fulfill the requirement of physical crosslinking. Therefore, researchers turned to discovering natural building blocks, leading to a bunch of supramolecular materials with advantages such as facile preparation, robustness and low cost.<sup>35</sup>

### 2.1. Hydrogen bonding

H-bonding is one of the most fundamental interactions facilitating the adhesion ability of polyphenol towards multiple surfaces. A large number of phenyl groups existing in TA enable it to couple to a vast majority of molecules containing a carboxyl group, hydroxyl group, amino group, ether linkage, fluorine atom, N-containing heterocyclic residues, sulfonate or phosphate through hydrogen bonding.<sup>36</sup> As TA derivatives bind to a given surface through hydrogen bonding, bidentate or tridentate hydrogen bonds could be formed owing to the catechol or pyrogallol groups. Such interactions are stronger than single-ligand hydrogen bonding, which means that a TA crosslinked material could be used as an underwater adhesive to adapt to an ever-changing operational environment.<sup>37</sup> Natural polymers, such as collagen, elastin, gelatin, and chitosan, or synthetic polymers such as poly(vinyl alcohol) (PVA), poly(ethylene glycol) (PEG), poly(vinylpyrrolidone) (PVP) and so on, could be cross-linked by TA through hydrogen bonding for biomedical applications. One of the advantages of such combinations is that strong interactions between TA and polymers could resist enzymatic degradation caused by collagenase or



**Table 1** Versatile routes leading to a TA-based polymeric network, through either physical crosslinking or chemical crosslinking

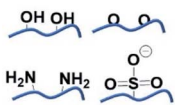
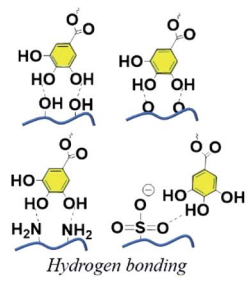
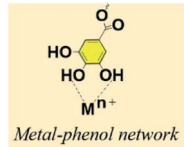
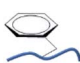
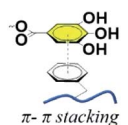

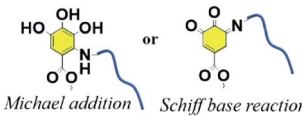

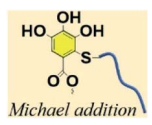
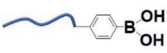
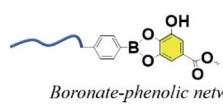
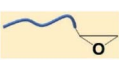
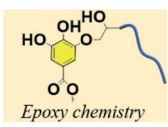
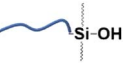
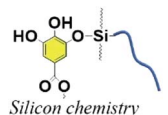

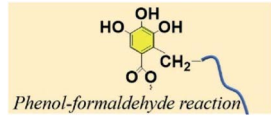

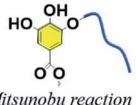

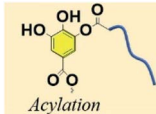

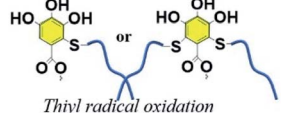
Entries for physical crosslinking	Reagent or substrate	TA based network
1		 <i>Hydrogen bonding</i>
2	$M^{n+}$	 <i>Metal-phenol network</i>
3		 <i><math>\pi</math>-<math>\pi</math> stacking</i>
Entries for chemical crosslinking	Reagent or substrate	TA based network
1		 <i>Michael addition</i> or <i>Schiff base reaction</i>
2		 <i>Michael addition</i>
3		 <i>Boronate-phenolic network</i>
4		 <i>Epoxy chemistry</i>
5		 <i>Silicon chemistry</i>
6		 <i>Phenol-formaldehyde reaction</i>
7		 <i>Mitsunobu reaction</i>

Table 1 (Contd.)

Entries for chemical crosslinking	Reagent or substrate	TA based network
8		 Acylation
9		 Thiyl radical oxidation

hyaluronidase.<sup>38</sup> It should be noted that supramolecular assemblies of TA-polymers *via* hydrogen bonding are highly pH-dependent, which further influences the mechanical properties and stability of the resulting networks. Under acidic conditions, the catechol and pyrogallol groups of TA are mainly protonated, becoming desirable hydrogen donors readily interacting with hydrogen-accepting building blocks. Under neutral conditions, the catechol and pyrogallol groups of TA prefer to be ionized, causing the dissociation of H-bonds between hydrogen-accepting building blocks and TA. A further increase in pH value gives rise to an unstable TA-polymer complex since the polyphenol groups are oxidized to the quinone form under ambient conditions.<sup>39</sup>

As to a TA-PVA complex, a partially crosslinked network could be obtained at pH values ranging from 3 to 4, which could form a semitranslucent hydrogel after a few freeze-thaw cycles. The resulting TA-PVA hydrogel presented better elasticity and a more yellow color accompanied by an increase in the TA mass ratio during hydrogel preparation, as can be seen in the work provided by Hong.<sup>40</sup> A fully crosslinked TA-PVA network could be obtained when the pH value was further decreased to 2,

which was unstable in water and precipitated as a bulk plastic-like dry polymeric material, as evidenced by Niu *et al.* (Fig. 2).<sup>41</sup> Owing to the high density of hydrogen bonds, this polymer composite had a toughness of 354 MJ m<sup>-3</sup> along with a tensile strength of *ca.* 104.2 MPa and a Young's modulus of *ca.* 3.53 GPa. The intramolecular interaction between TA and PEG has also been involved to improve the mechanical properties of polymeric composites. Recently, Lee *et al.* successfully fabricated hyaluronic acid (HA)-TA hydrogels, in which TA was incorporated into the hydrogel network through hydrogen bonding with ether groups of polyethylene glycol diglycidyl ether (PEGDE).<sup>42</sup> They also proved that the TA-based hydrogel network could fulfill demands over a prolonged clinical period as well as physiological functions with antioxidant, antibacterial and anti-inflammatory properties. Moreover, as reported in the work of Du *et al.*, a hybrid hydrogel containing PEG, quaternized chitosan (QCS) and TA (PEGDA/QCS/TA) was developed based on mussel-inspired chemistry.<sup>43</sup> The incorporation of TA *via* multiple hydrogen bonding with PEG enabled properties such as anti-swelling, high mechanical strength, antimicrobial and excellent adhesive properties to versatile surfaces.

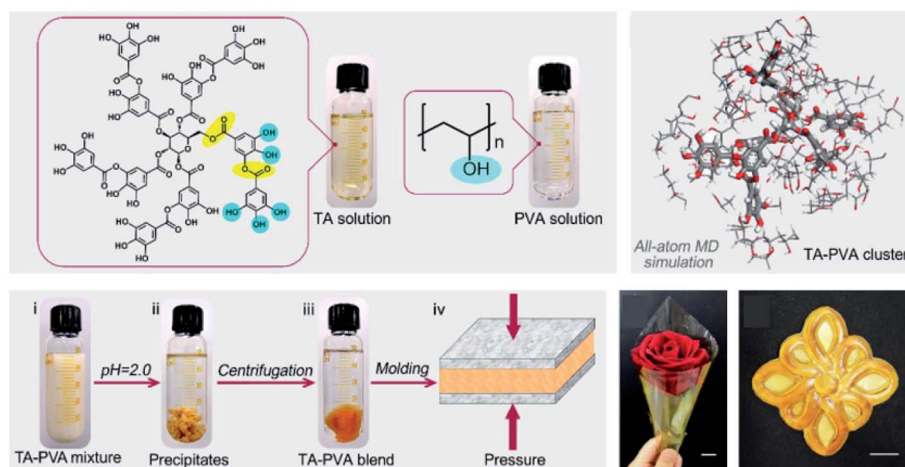


Fig. 2 Schematic illustration of the preparation process of TA-PVA composites. Reproduced from ref. 41 with permission from the American Chemical Society, copyright 2020.





## 2.2. $\pi$ - $\pi$ stacking

A combination between graphene and TA was desirable for numerous researchers in fields such as dye adsorption, material reinforcement and three-dimensional (3D) graphene macrostructures.<sup>44,45</sup> Over the past few years, graphene has gained substantial attention from researchers owing to its high tensile strength, huge specific area, distinguished electrical conductivity and gas tightness.<sup>46,47</sup> Nonetheless, graphene nanosheets generally tend to aggregate and restack with each other because of strong  $\pi$ - $\pi$  stacking, hydrophobic adsorption and van der Waals forces, leading to hindrance of the large accessible interfaces of graphene sheets.<sup>48</sup> Pointing to this issue, Liu and Wang *et al.* reported that natural phenolic acids such as TA could promote the self-assembly of graphene nanosheets into 3D structures.<sup>49,50</sup> In these cases, TA not only adsorbed firmly onto the graphene surface *via*  $\pi$ - $\pi$  stacking, endowing graphene with water dispersion stability, but also reduced graphene oxide (GO) into reduced graphene oxide (RGO) for enhanced chemical stability.

Moreover, catechol and pyrogallol moieties of TA have features such as tissue adhesion, ready chemical reactivity and metal ion reduction, making TA a good interface stabilizer for polymer/graphene hybrid materials.<sup>51</sup> For instance, Liu *et al.* developed a new chitin-based composite hydrogel reinforced by TA-modified reduced GO (TRGO) prepared *via* a facile freezing-thawing approach (Fig. 3). This TRGO reinforced hydrogel exhibited excellent adsorption capacity towards Congo red (CR).<sup>44</sup> Zhao *et al.* synthesized a TA-modified graphene/SiO<sub>2</sub> hybrid filler, which was proved to be a facile route leading to high-performance rubber nanocomposites.<sup>52</sup> TA-GO composites can also incorporate noble metal nanoparticles due to the reducing property of polyphenols, thus providing TA-GO-based material with catalytic or antibacterial performance. In the work provided by Luo *et al.*, a rapid, low-cost, and environmentally-friendly method was developed to obtain gold nanoparticle (Au NP) modified graphene hydrogel by taking advantage of TA-based reducibility.<sup>53</sup> This Au NP modified graphene hydrogel

(Au@TA-GH) manifested greatly advanced catalytic activities over unsupported and other polymer-supported Au NPs in the process of methylene blue (MB) reduction. Similarly, Wang *et al.* presented an ultralight 3D graphene hybrid aerogel containing TA, GO and modified polyaspartamide [PolyAspAm(EDA/EA)].<sup>45</sup> The corresponding hydrogel is considered to be formed *via* various interactions such as hydrogen bonding, covalent bonding, and weak  $\pi$ - $\pi$  interactions. These 3D polymer-graphene composite materials containing TA-mediated noble metal nanoparticles are promising for use as new interfacially active materials for a wide range of long-term catalytic applications.

Apart from TA-functionalized graphene, non-covalently functionalized carbon nanotubes (CNTs) *via*  $\pi$ - $\pi$  interactions can also be obtained using TA as the stabilizer, which enhances the water dispersion property of CNTs in the polymeric network. He *et al.* developed a conductive hydrogel by incorporating TA-coated CNTs into a polyvinyl alcohol (PVA) hydrogel matrix, in which water and glycerol were used as a dispersion medium (Fig. 4).<sup>54</sup> The resulting TA-CNT-glycerol-PVA (TCGP) hydrogel exhibited excellent freezing-resistance properties ( $-30$  °C), long-term moisture retention performance (10 days), and outstanding strain or pressure sensitivity. Additionally, the TCGP hydrogel could be used not only as a wearable skin sensor for the tracking of multiple human motions, but also as a probe for detecting human electrophysiological information even in a harsh environment. In the work provided by Tan *et al.*, a photoactive TA (pTA) was first synthesized *via* the ring-opening reaction between TA and glycidyl methacrylate (GMA), and then CNTs were coated with pTA *via*  $\pi$ - $\pi$  interactions to obtain UV-curable carbon nanotubes (pTA/MWCNTs).<sup>55</sup> Applied as a filler, this material was effective for the reinforcement of acrylated epoxidized soybean oil (AESO).

## 2.3. Metal-phenol network (MPN)

TA-based metal-organic networks have aroused widespread attention because of their diverse properties, including (i) pH

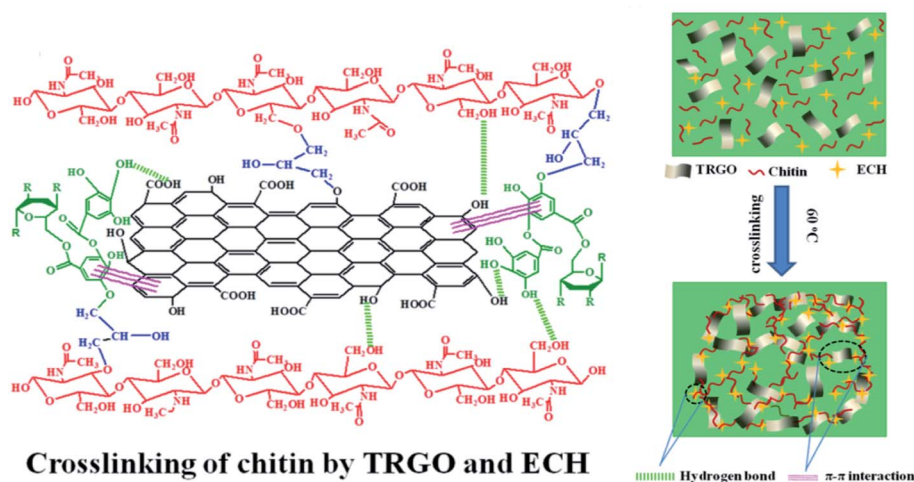


Fig. 3 Preparation and the crosslinked network of chitin-TRGO composite hydrogels. Reproduced from ref. 44 with permission from Springer, copyright 2020.

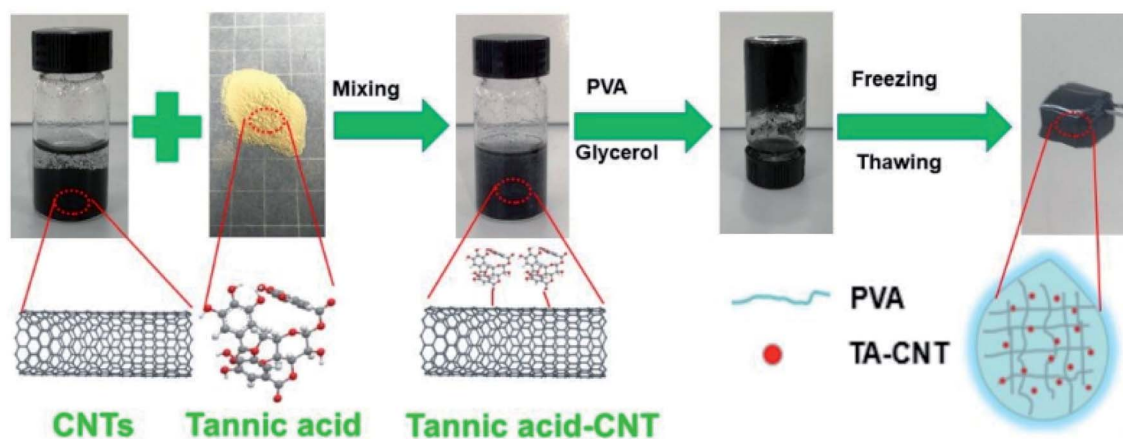


Fig. 4 The preparation of TA-CNT-glycerol-PVA hydrogel for moist-electric generation. Reproduced from ref. 54 with permission from the Royal Society of Chemistry, copyright 2020.

and temperature responsiveness derived from the supramolecular nature of dynamic coordination bonds, (ii) the combined biomedical properties of both metals and polyphenols, (iii) controlled crosslinking density achieved by variation of the

metal/polyphenol mass ratio.<sup>56</sup> These supramolecular materials have great potential in drug vehicles,<sup>57</sup> optical materials,<sup>58</sup> chemical sensors,<sup>59</sup> gas adsorption,<sup>60</sup> power storage,<sup>61</sup> and catalysts.<sup>62</sup> Specifically, TA and  $\text{Fe}^{\text{III}}$  were usually chosen as the

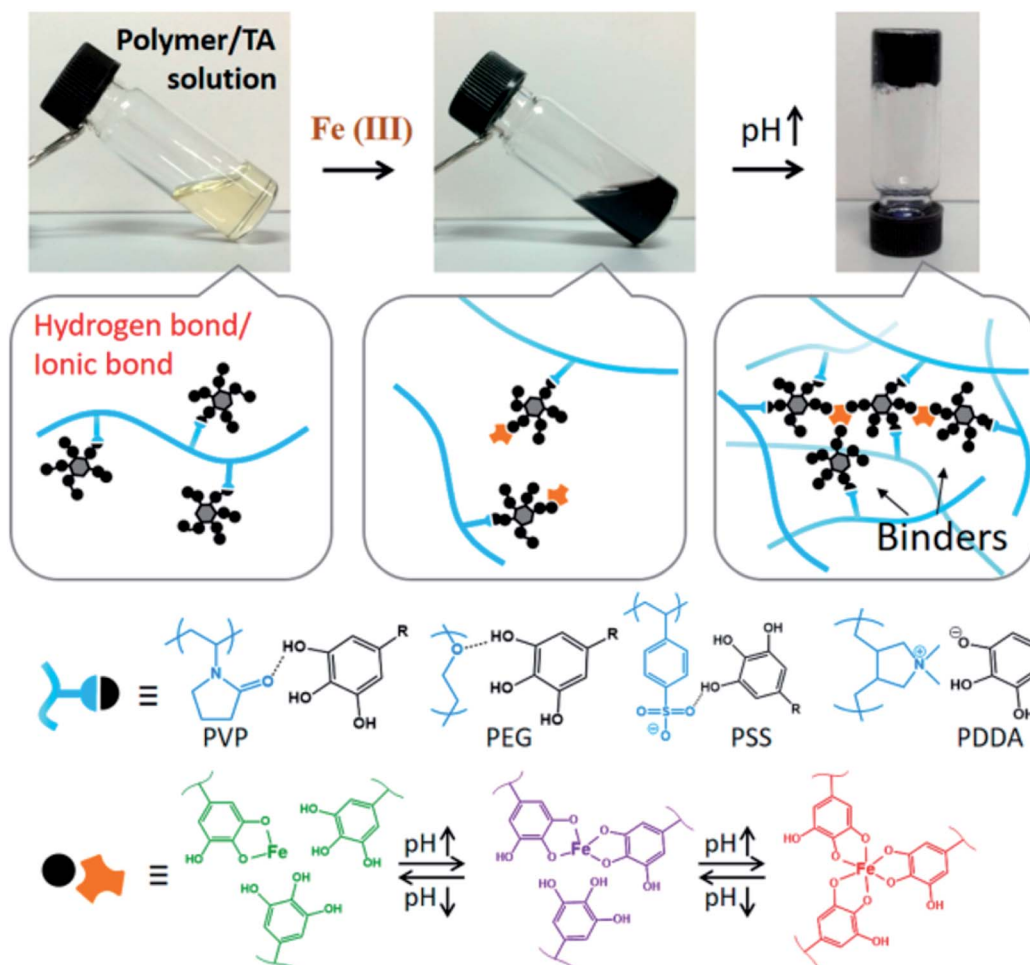


Fig. 5 Formation mechanism of TA-polymer hydrogels based on polymer/TA/ $\text{Fe}^{\text{III}}$ . Reproduced from ref. 68 with permission from the American Chemical Society, copyright 2017.



organic ligand and the inorganic crosslinker, respectively. Caruso *et al.* proposed that the MPN network formed between  $\text{Fe}^{\text{III}}$  and TA is pH-dependent. At pH 2.0–3.0, most of the pyrogallol moieties were protonated, which gave rise to rapid destabilization of coordination bonds and disassembly of the network. The stability of the TA- $\text{Fe}^{\text{III}}$  complex increased at pH > 7 since TA could chelate with each  $\text{Fe}^{\text{III}}$  ion to form a stable octahedral complex.<sup>63,64</sup> Additionally, other metals, including Al, V, Cr, Mn, Co, Ni, Cu, Zn, Zr, Rh, were coordinated with TA to form functional MPN networks on particulate substrates. For instance, the  $\text{Rh}^{\text{III}}$ -TA complex possessed a catalytic function for the hydrogenation of quinolone.<sup>65</sup> The  $\text{Mn}^{\text{II}}$ -TA complex exhibited the highest relaxivity  $r_2$ , which is of the order of  $60 \text{ s}^{-1} \text{ mm}^{-1}$  and generally sufficient for *in vivo* magnetic resonance imaging.<sup>66</sup>

Straightforward crosslinking of a TA-polymer complex into bulk material is still a challenge since the strong tendency for supramolecular interactions often leads to partial coacervation rather than a homogeneous bulk material.<sup>67</sup> Balanced control over the hydrogen bonding or ionic interactions between polymers and TA molecules should be considered, which can be solved by adding metal ions to TA-polymer composites. Based

on the above concept, Fan *et al.* functionalized polymers such as polyvinylpyrrolidone (PVP), poly(ethylene glycol) (PEG), poly(sodium 4-styrenesulfonate) (PSS), and poly(dimethyldiallylammonium chloride) (PDDA) with catechol/pyrogallol groups by TA and  $\text{Fe}^{\text{III}}$  sequentially (Fig. 5).<sup>68</sup> The special performance of such hydrogels includes pH-stimulated assembly, rapid self-healing, and radical scavenging abilities. Since TA can affect the biological availability or activity of metal ions through chelation, the pH-sensitive property of MPN can also be utilized to construct smart biomaterials. Ninan *et al.* integrated the advantageous properties of TA,  $\text{ZnCl}_2$  and carboxylated agarose to fabricate a series of pH-sensitive hydrogels for wound healing (Fig. 6).<sup>69</sup> At acidic pH, the polyphenol groups of TA were highly protonated and relatively few phenolate binding sites were allowed to complex with zinc ions. As the pH rose, deprotonation of TA occurred, triggering the formation of an MPN network. The hydrogels could release TA in a pH-dependent manner, which showed great potential as wound dressing. Li *et al.* also used  $\text{Fe}^{\text{III}}$  to stabilize the interaction between TA and polyaniline, thus forming a stable hydrogel for a carbon aerogel precursor.<sup>70</sup> Li *et al.* synthesized a new dual-network self-healing hydrogel, in which  $\text{Al}^{\text{III}}$  was

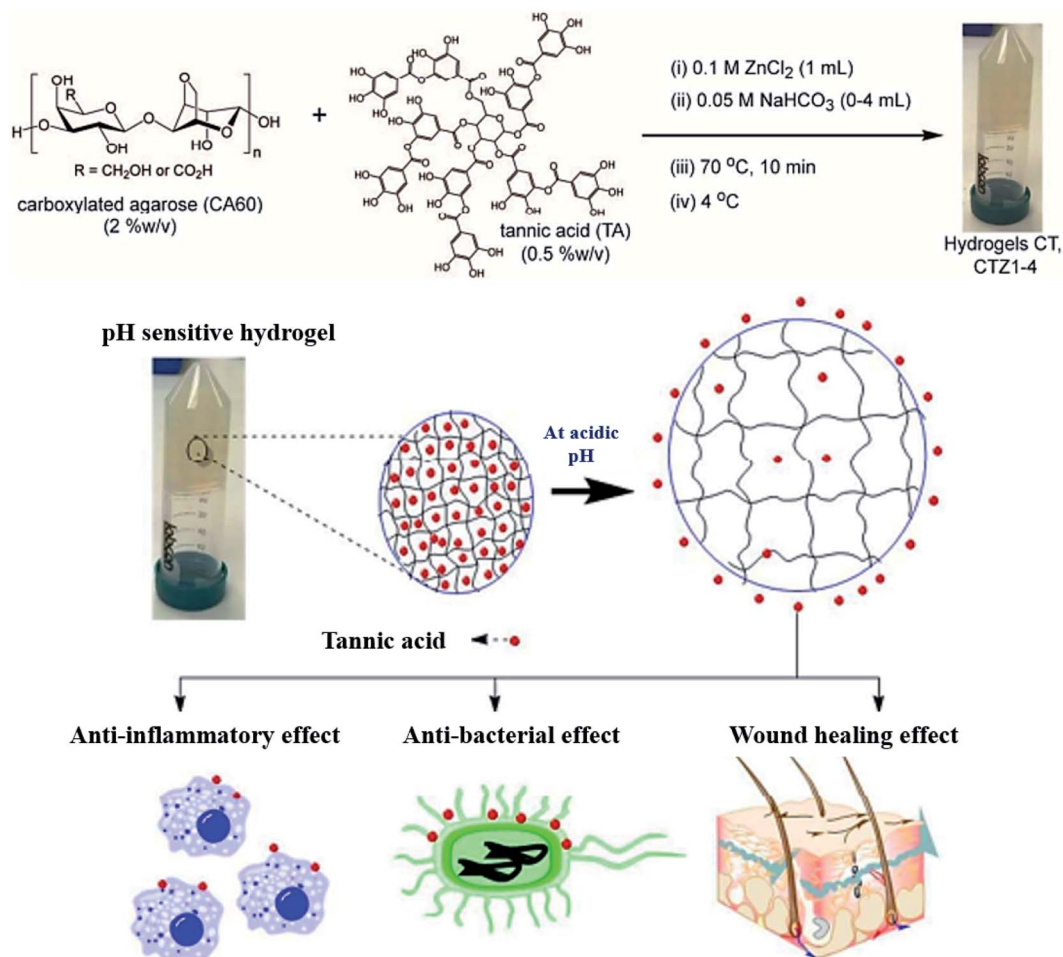


Fig. 6 Anti-microbial and anti-inflammatory pH-sensitive TA-based composite hydrogels for wound healing. Reproduced from ref. 69 with permission from the American Chemical Society, copyright 2016.



employed to stabilize the TA–poly(acrylic acid)–chitosan complex.<sup>71</sup>

phenol–aldehyde reaction, phenolic acylation and radical oxidation have been utilized by various researchers for extensive uses.

### 3. Chemical crosslinking

The increasing interest in phenolic molecules is ascribed to their broad scope of chemical properties and multivalent reactive sites.<sup>6,7,72</sup> In reference to the adhesive property of mussels, polydopamine (PDA) has been applied in surface modification to tailor nanoparticles, membranes or hydrogels at multiple scales because of their excellent adhesion ability, mild modification conditions without pollution, and versatile secondary reaction types.<sup>17,73</sup> TA, with 2–12 gallic units per molecule, also has similar characteristics of chemical reactivity to PDA. Numerous chemical crosslinking methods including phenol–amine Michael/Schiff base reaction, phenol–thiol Michael addition, phenol–boronic acid reaction, phenol–epoxy ring-opening reaction, phenol–alcohol Mitsunobu reaction,

#### 3.1. Phenol–amine Michael and Schiff base reaction

A weakly basic condition (at pH values of ~8–8.5) can trigger successive crosslinking between phenols and amines to enhance the cohesion of catechol or pyrogallol moiety containing adhesive.<sup>74</sup> Although the catechol–amine reaction type is recognized as either a Michael addition or a Schiff base process, it is still uncertain which mechanism is prevalent in a given case.<sup>75</sup> The work reported by Qiu *et al.* suggested that Michael addition occurred under aerobic and mild alkaline conditions with both primary and secondary amines preferring to link with catechol to form oligomers. According to the results of molecular simulations, Michael addition products are prevalent for both aromatic and aliphatic amines with catechol, supporting the fact that the corresponding co-deposited

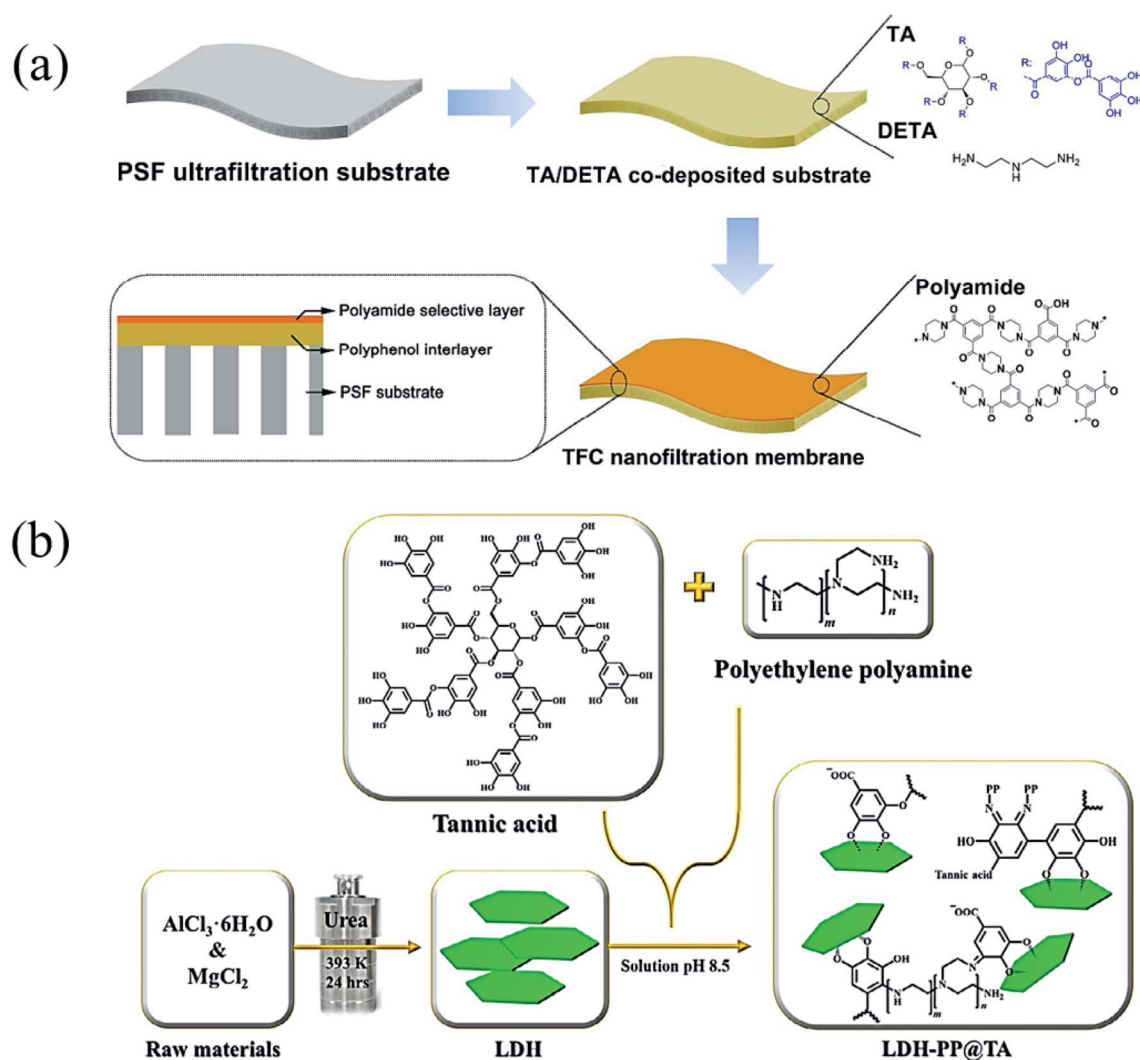
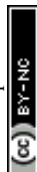


Fig. 7 (a) A polyphenol interlayer coated onto a polysulfone (PSF) ultrafiltration membrane. Reproduced from ref. 80 with permission from the American Chemical Society, copyright 2016. (b) TA and polyethylene polyamine were co-deposited onto MgAl-layered double hydroxide (LDH). Reproduced from ref. 81 with permission from the Elsevier, copyright 2018.





coatings are durable under various operating environments.<sup>76</sup> Whereas in the presence of strong oxidants (*e.g.*  $\text{NaIO}_4$ ), TA can be oxidized to yield a quinone-rich structure that is able to react with amines following the Schiff base mechanism.<sup>77</sup>

The products of the phenol/amine Michael/Schiff base reaction have been recognized as valuable in versatile applications because of their uniform coating or surface modification property.<sup>78</sup> In contrast to dopamine (DA), TA and polyamines are much more stable in an ambient atmosphere, possessing the features of low cost and convenient storage. Furthermore, this reaction strategy is prevalent in biomimicking membranes since it has non-toxic or low-cost raw materials, controllable crosslinking density and rapid deposition.<sup>79</sup> In an appropriate case, Zhang *et al.* demonstrated that TA are capable of forming coatings similar to polydopamine (PDA) on various surfaces *via* co-deposition with amino-containing polymers or organic molecules (Fig. 7a).<sup>80</sup> In detail, polyphenol coatings were obtained by the phenol/amine Michael reaction between TA and diethylenetriamine (DETA) on polysulfone ultrafiltration membranes for improved water wettability and enhanced nanofiltration performance. With the aim of improving the adsorption capacity of heavy metal ions, Huang *et al.* modified MgAl-layered double hydroxide (LDH) *via* co-deposition of polyethylene polyamine (PP) and tannic acid (TA) (Fig. 7b).<sup>81</sup> With its combination of polyphenol chemistry and nitrogen-rich binding sites, the as-prepared LDH-PP@TA could be used to adsorb copper(II) ions from wastewater.

Natural biopolymers such as silk fiber (SF), gelatin, lysine and chitosan are polyamides that could also be modified by tannic acid *via* the phenol-amine Michael/Schiff base reaction. The incorporation of TA as a commercially available chemical

crosslinker, molecular glue, and antibacterial agent granted polymer-TA conjugates with a bioadhesive property.<sup>82</sup> In the work reported by Pang *et al.*, low-cost dopamine analogues (alkali lignin as well as TA) were used to develop a reinforced silkworm SF *via* a Schiff base reaction between polyphenol moieties and amine groups, which formed a network mimicking “reinforced concrete” (Fig. 8a).<sup>83</sup> As a result, the lignin-coated and TA-coated SFs are preferable for strengthening SF due to the more condensed crosslinking sites as well as lower cost in contrast to PDA. TA-modified gelatin bioadhesives had advantages such as ready scalability, relatively low cost and the elimination of concerns about neurological side-effects caused by DA. Recently, Ge fabricated dual cross-linked gelatin-oxidized tannic acid- $\text{FeCl}_3 \cdot 6\text{H}_2\text{O}$  (DC-GT/OTA/ $\text{Fe}^{\text{III}}$ ) hydrogels in which phenol-amine and MPN crosslinking strategies were used.<sup>84</sup> Moreover, Guo *et al.* designed a facile, straightforward Michael addition reaction method to produce TA-based bioadhesives, in which tannic acid and gelatin interacted under oxidizing conditions.<sup>85</sup> Similarly, Zhao *et al.* created TA-modified gelatin hydrogels *via* both supramolecular interactions and covalent bonding under a strong oxidant (Fig. 8b).<sup>86</sup> The outstanding viscoelasticity, thermal sensitivity, and macroporosity granted the present hydrogel promising application prospects in wound healing, tissue adhesion and drug loading.

### 3.2. Phenol-thiol Michael addition

Polyphenol chemistry accounts for the improved adhesion, macromolecular network formation, and mechanical strengthen in reference to mussel adhesive proteins.<sup>87</sup> Catechol or pyrogallol groups could be easily transferred to *o*-quinone in the presence of an oxidase or in alkaline seawater.<sup>88</sup>

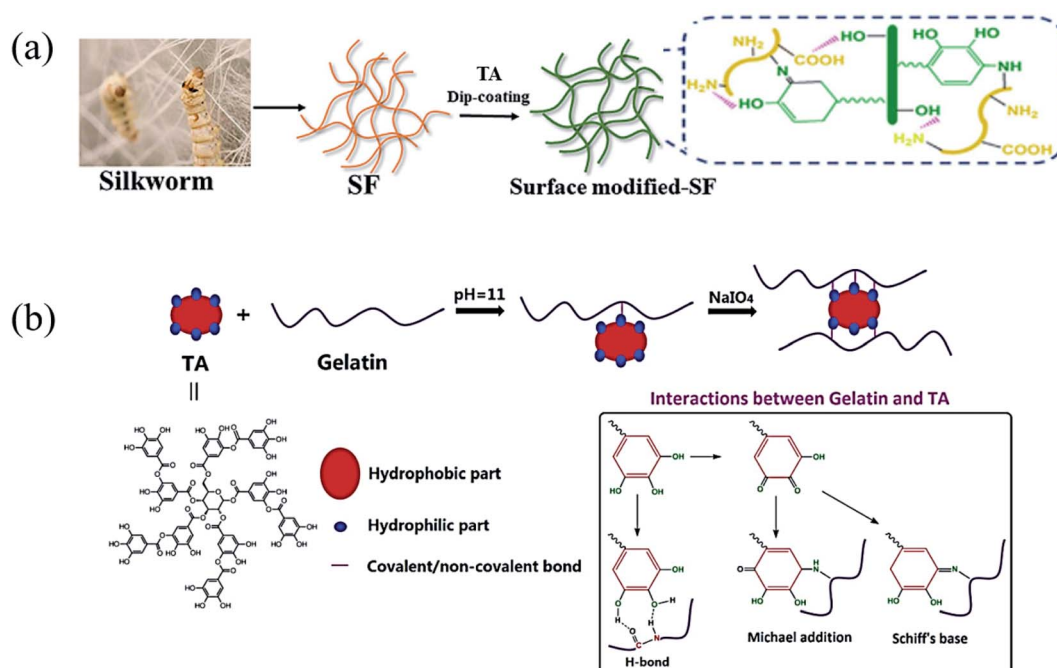
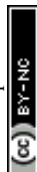


Fig. 8 (a) Silk fiber was modified by TA. Reproduced from ref. 83 with permission from Wiley-VCH, copyright 2020. (b) Crosslinking mechanism of oxidated TA and gelatin under alkaline conditions. Reproduced from ref. 86 with permission from Wiley-VCH, copyright 2019.



Nucleophilic reactions such as quinone–phenol dismutation, Schiff base reaction or Michael addition occur between *o*-quinone and various substrates containing catechol, amine or thiol groups.<sup>89,90</sup> The phenol–thiol Michael addition between TA and thiol-bearing polymers has generally been utilized in the construction of antifouling membranes or surfaces with desired properties.<sup>91</sup>

In an effort to reduce environmental pollution, polymer brushes, whether hydrophilic or amphiphilic, have been designed to construct nondepleting coatings for antifouling membranes.<sup>92</sup> Therefore, the development of new surface functionalization techniques with green chemistry and easy processing is in line with current interests and concerns. In comparison to dopamine or dopa-derivatives, TA is generally widely acknowledged as safe (GRAS) by the U.S. Food and Drug Administration (FDA), which ensures a “greener” surface-modification technique.<sup>93</sup> In the work proposed by Pranantyo *et al.*, multilayer polymeric layer anchors on stainless steel substrates were achieved by deposition of TA and then tethered hyperbranched polyglycerols bearing terminal thiol moieties (HPG-SH).<sup>94</sup> In terms of qualitative and quantitative assays of settlement of the microalgae *Amphora coffeaeformis*, this polymeric anchor was proved to have low fouling characteristics. A similar method could be seen in the work provided by Xu *et al.*<sup>95</sup>

### 3.3. Phenol–epoxy ring opening reaction

In an age of rapid petroleum consumption, the world is currently encountering issues such as climbing oil prices, the greenhouse effect and stacks of nondegradable plastic. People urgently need to explore “greener” industry for sustainable uses.<sup>96</sup> However, until now petrochemically-derived acrylate polymers have been used predominantly in many applications, which have been predicted to be exhausted in the foreseeable future.<sup>97</sup> Reproducible resources such as degradable chemicals and oils originating from plants have already been used in the tannery industry both as resins by self-polycondensation and as raw material crosslinkers for coating resins. TA, a low-cost compound, possesses multiple chemical binding sites as well as multiple aromatic rings, ensuring a high  $T_g$  green epoxy resin.<sup>98–100</sup>

Previous studies have proved that under certain heating conditions, the pyrogallol groups on TA are capable of triggering ring-opening of oxirane rings, making TA a chemical hardener for epoxy material.<sup>101,102</sup> Recently, Feng *et al.* proposed a facile method to prepare a TA-hardened epoxy resin, in which TA was applied as a multifunctional crosslinking agent for diglycidyl ether of bisphenol A (DGEBA) (Fig. 9).<sup>103</sup> Previous researchers revealed that the reactivity of the outer-layer hydroxyl groups in TA have a higher chance of reacting with oxirane rings than inner-layer hydroxyl groups because of the

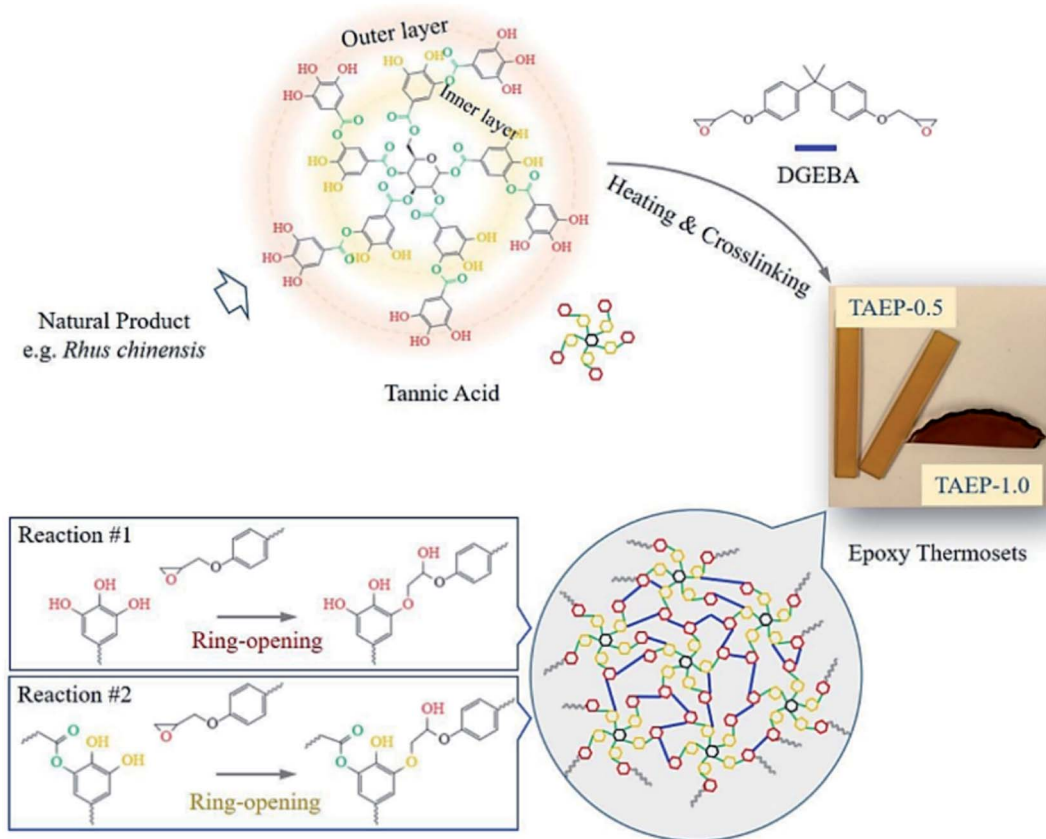


Fig. 9 The polymerization between TA and epoxy monomer (DGEBA) to produce tunable thermosets. Reproduced from ref. 103 with permission from the American Chemical Society, copyright 2020.



steric hindrance of the dendritic structures of TA.<sup>98</sup> Thanks to the multiple binding sites and special topological structure of TA, the resulting epoxy thermosets demonstrated a hierarchical network structure with desirable mechanical strength and tunable functionalities, such as shock absorption, shape memory, and sustainable uses. Similar work has also been proposed by Handique *et al.*<sup>104</sup> and Baruah *et al.*,<sup>105</sup> which revealed that TA could potentially replace novolac resins in a green way and alleviate the health and environmental burdens of undegradable epoxy material synthesis.

### 3.4. Silanol-phenol condensation

Organic-inorganic hybrid polymers could be obtained *via* silanol-phenol condensation. This process normally consists of two steps: (i) silane/siloxane precursors are first hydrolyzed to form silanol in water. (ii) Silanol reacts with the hydroxyl groups of polyphenols. In the earliest studies, silanol-phenol polymeric networks were used for fabricating superhydrophilic organic-inorganic hybrid membranes *via* the co-deposition of polyphenols and silanes.<sup>106</sup> Furthermore, Sa *et al.* proved that silanol would tend to react with the hydroxyl groups of dopamine, which are much more active than the hydroxyl groups belonging to PDA.<sup>107</sup> Analogous to dopamine, the hydroxyl groups of TA are able to react with the Si-OH groups of silanol under mild conditions.

In the work of He *et al.*, TA was applied as a stabilizer to disperse graphene in aqueous solution *via*  $\pi$ - $\pi$  stacking to form graphene-TA hybrids. Subsequently,  $\gamma$ -(2,3-epoxypropoxy) propyltrimethoxysilane (KH560) was added to modify the surface of graphene-TA *via* silanol-phenol condensation to obtain an organic-inorganic hybrid anti-corrosion coating.<sup>108</sup> Inspired by the phenomenon that polyphenols in red wine or tea tend to deposit onto flexible surfaces or given containers, an alcohol precursor  $\gamma$ -(2,3-epoxypropoxy) propyltriethoxysilane (KH561) was involved in constructing the polyphenol-silanol network. Chen *et al.* developed TA-KH561 copolymer (TA561) under mild

conditions for a strong adhesion material and wound healing (Fig. 10).<sup>109</sup> Under continuous heating, a sol-gel transition occurred to form solid TA561 because of the formation of a TA crosslinked polysiloxane network. TA561 copolymer could not only be applied as an adhesive for materials in daily use, but also manifested antibacterial activity in the wound healing process.

### 3.5. Boronate-phenolic network (BPN)

Currently, dynamic covalent interactions have been extended to prepare hydrogels with programed degradation and cargo release behaviour by exploiting the stimuli-responsive nature of dynamic covalent bonds.<sup>110-112</sup> For instance, boronic esters are normally synthesized *via* the esterification reaction between boronic acids and cis-1,2 or cis-1,3 diols, which could reversibly dissociate under acidic conditions.<sup>113</sup> It has been proved that boronic esters are stable under physiological conditions with no or extremely little side effects.<sup>114</sup> Because of the favorable *syn-peri*-planar configuration of the aromatic hydroxyl groups as well as their electron-donating features, phenolic compounds are excellent building blocks to construct boronate ester networks.<sup>115</sup> Coincidentally, TA usually consists of a central glucose surrounded by 10 galloyl units end-capped with aromatic triols, and the tip of the branch units feature either a catechol (1,2-diol) or a 1,3-diol. It is reasonable to construct copolymers *via* the reaction between TA and boronic acid derivatives.

Several research groups have reported a series of pH-responsive capsules prepared by the multistep layer-by-layer (LbL) assembly of boronate-functionalized macromolecules with polyelectrolytes.<sup>116,117</sup> However, none of these capsules are stable and responsive to cis-diols under alkaline pH environments (e.g., pH 9–11), which is an obstacle in practical medical applications. Facing this issue, Guo *et al.* reported a dual-responsive capsule system toward pH and cis-diol through the boronate-phenolic network formed between phenylboronic

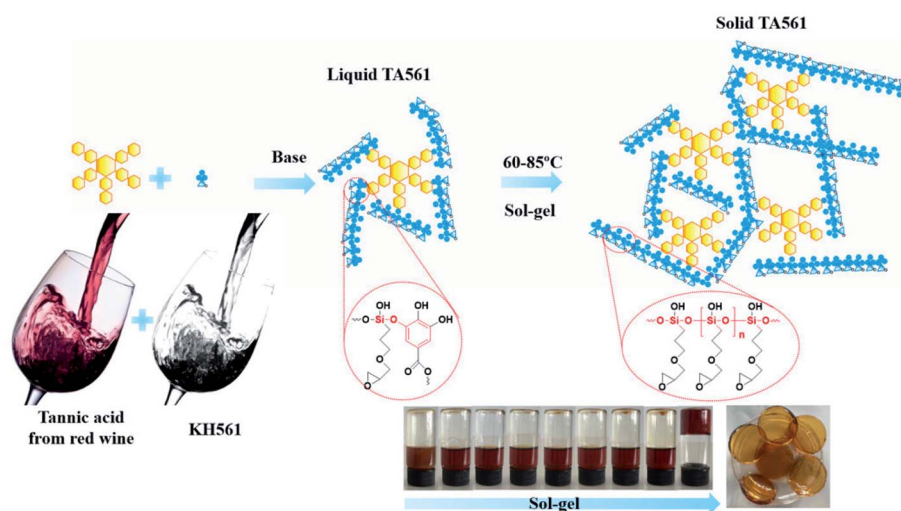


Fig. 10 Synthetic production of TA-KH561 copolymer under mild conditions. Reproduced from ref. 109 with permission from the Royal Society of Chemistry, copyright 2021.

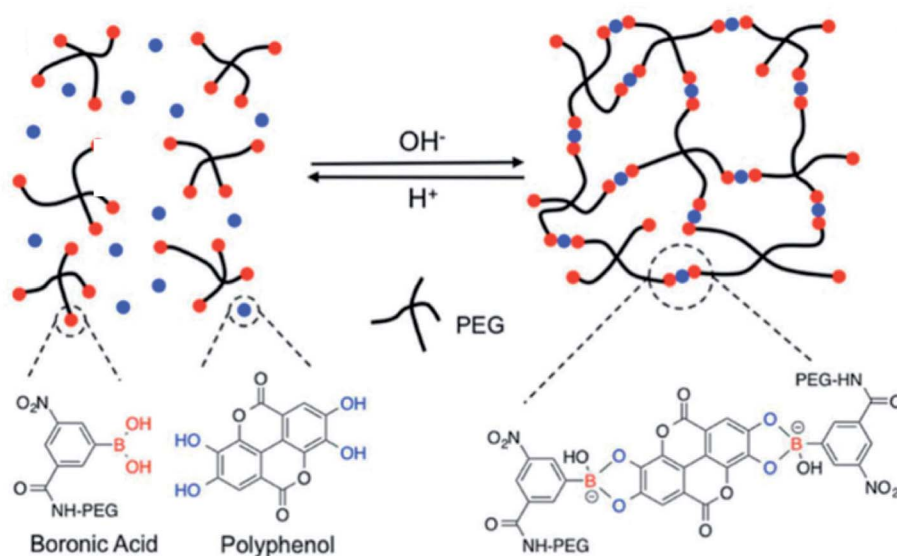


Fig. 11 Dynamic nature and pH-responsive network formed between boronic acid-terminated PEG and polyphenols. Reproduced from ref. 119 with permission from the Royal Society of Chemistry, copyright 2018.

acid (BDBA) and a polyphenol (TA) on particulate templates.<sup>118</sup> At alkaline pH, the BDBA-TA composites turned out to be stable boronate ester networks. Exploring the pH responsiveness and dynamic nature of complexes between boronic acid-terminated PEG and polyphenols, Huang *et al.* created injectable BPN hydrogels (Fig. 11).<sup>119</sup> In this procedure, the polyphenol acted both as therapeutic agent and crosslinker, and a sol-gel transition occurred when a precursor solution containing boronic acid-terminated polymer and polyphenol was injected *in vivo*. Additionally, Montanari *et al.* developed a pH-responsive, hyaluronic acid (HA)-based nanoparticle system for the encapsulation of TA.<sup>120</sup> Above all, these BPN-based materials are promising for application as smart, long-acting, and targetable therapeutic agents for cancer.

### 3.6. Phenol-alcohol Mitsunobu reaction

The Mitsunobu reaction, essentially a significant dehydration reaction, generally involves the coupling between a primary or

secondary alcohol and an acidic pronucleophile (NuH) catalyzed by a redox combination of a trialkyl or triarylphosphine and a dialkyl azodicarboxylate. This reaction has gained extensive use in various synthetic procedures because of its wide scope, stereospecificity and mild reaction conditions.<sup>121</sup> TA, with a  $pK_a$  of 10, could be exploited as an acidic nucleophile as well as a crosslinker. Chen *et al.* proposed a covalent-crosslinking method in which TA was subjected to direct PEGylation *via* Mitsunobu polymerization (Fig. 12).<sup>122</sup> This phenol-alcohol reaction was conducted under mild conditions (0–25 °C) in the presence of  $PPh_3$ /diisopropyl azodicarboxylate (DIAD). TA-PEG hydrogel could not only chelate  $Fe^{III}$  to form a composite hydrogel, but also had the ability to reduce  $Au^{III}$  and  $Ag^I$  ions rapidly within 5–10 min to produce the corresponding nanoparticles. Antimicrobial measurements suggested that TA-PEG hydrogel as well as TA-PEG-AgNPs hydrogel showed excellent antibacterial activity against *S. aureus* and *E. coli*.

#### Synthetic Route



Fig. 12 Direct PEGylation of TA under mild conditions to construct a TA-PEG hydrogel. Reproduced from ref. 122 with permission from the Royal Society of Chemistry, copyright 2021.





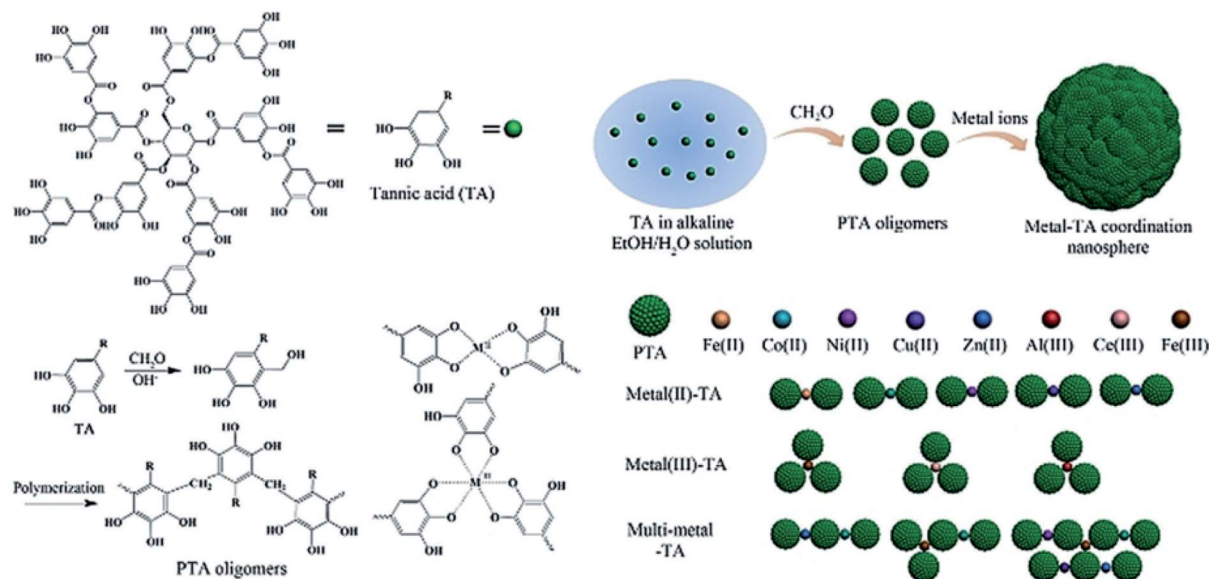


Fig. 13 The synthetic procedure and the proposed precipitation mechanism of TA-formaldehyde microspheres. Reproduced from ref. 123 with permission from Wiley-VCH, copyright 2018.

### 3.7. Phenol-aldehyde reaction

The pyrogallol groups of TA can also be crosslinked by formaldehyde just like phenolic resin. Wei *et al.* reported a method leading to TA-formaldehyde microspheres with uniform diameter as electrode materials (Fig. 13).<sup>123</sup> Similarly, with the aim of removing pollutants from industrial wastewater, Zhang *et al.* synthesized a Fe<sup>III</sup>-TA-formaldehyde polymer *via* a one-pot hydrothermal method, in which Fe<sup>III</sup> and formaldehyde were utilized as dual crosslinkers.<sup>124</sup> Owing to the polyphenol moieties, Fe<sup>III</sup>-TA-formaldehyde particles could efficiently trap methylene blue, Pb<sup>II</sup>, and Hg<sup>II</sup> from aqueous solution with rapid adsorption kinetics. Apart from the above TA-formaldehyde crosslinking method, Chen *et al.* employed TA-glutaraldehyde crosslinking for surface modification of melamine foam.<sup>125</sup> The nucleophilic centers of TA allow it to react with glutaraldehyde, providing the possibility of achieving a stable network as well as enhancing surface roughness.

### 3.8. Acylation of polyphenols

The acylation process incorporates the activation of acid groups belonging to polymer or monomer by a catalyst or continuous heating, followed by dehydration between the activated acid groups and hydroxyl groups.<sup>126</sup> In the work of Sahiner *et al.*, *N,N'*-carbonyldiimidazol was found to be an efficient catalyst for acylation of TA, offering some plus points including mild reaction conditions, very few byproducts, and low cost.<sup>127</sup> The acylation of polyphenols can also proceed without a catalyst. Recently, Guo *et al.* proposed that, under specific crosslinking conditions (80–120 °C, 1–3 days), the hydroxyl groups of TA can bridge citrate to obtain stable tannin-bridged hydroxyapatite (HA) bone composites for lumbar fusion.<sup>128</sup> Combining the merits of TA and citrate components, the obtained citrate-based tannin-bridged bone composites demonstrated increased compression strength, prolonged degradation behaviour,

enhanced biomineralization performance, excellent biocompatibility, and low cellular toxicity as well as considerable antibacterial properties.

### 3.9. Polyphenol-thiyl radical oxidation reaction

It should be noted that the reducing activity of TA is based on consecutive radical reactions, such as radical scavenging of harmful radicals originating from biomacromolecules under high temperature or ultraviolet irradiation. New stable compounds come into being *via* radical-scavenging reactions between TA and radical species derived from food or metabolic products.<sup>129</sup> Generally, TA was found to be applicable as a cooking ingredient for protein, in which a new polymeric network was formed by the breakage of the disulfide bonds and a polyphenol-thiyl radical oxidation reaction. Typically, improved dough properties could be achieved when the amount of TA added reached 0.03 g kg<sup>-1</sup> in bread making.<sup>130</sup> Above all, it can be concluded that the integration of TA and sulfur-rich molecules is a potential route to obtain crosslinked polymers for biomedical applications. Integrating the advantages of TA and polysulfur, Chen *et al.* synthesized a tannic acid-thioctic acid (TATA) hydrogel through a polyphenol-thiyl radical oxidation reaction (Fig. 14).<sup>131</sup> Owing to the chemical crosslinking as well as supramolecular assembly of the TATA matrix, the TATA hydrogel exhibited strong tissue adhesion, desirable biocompatibility, and biodegradability with minimal inflammatory response. Thus, the TATA hydrogel is promising for use as an injective tissue adhesive.

## 4. Applications of tannic-acid-crosslinked networks

The utilization of TA-functionalized networks can be found in various studies and the corresponding material categories cover

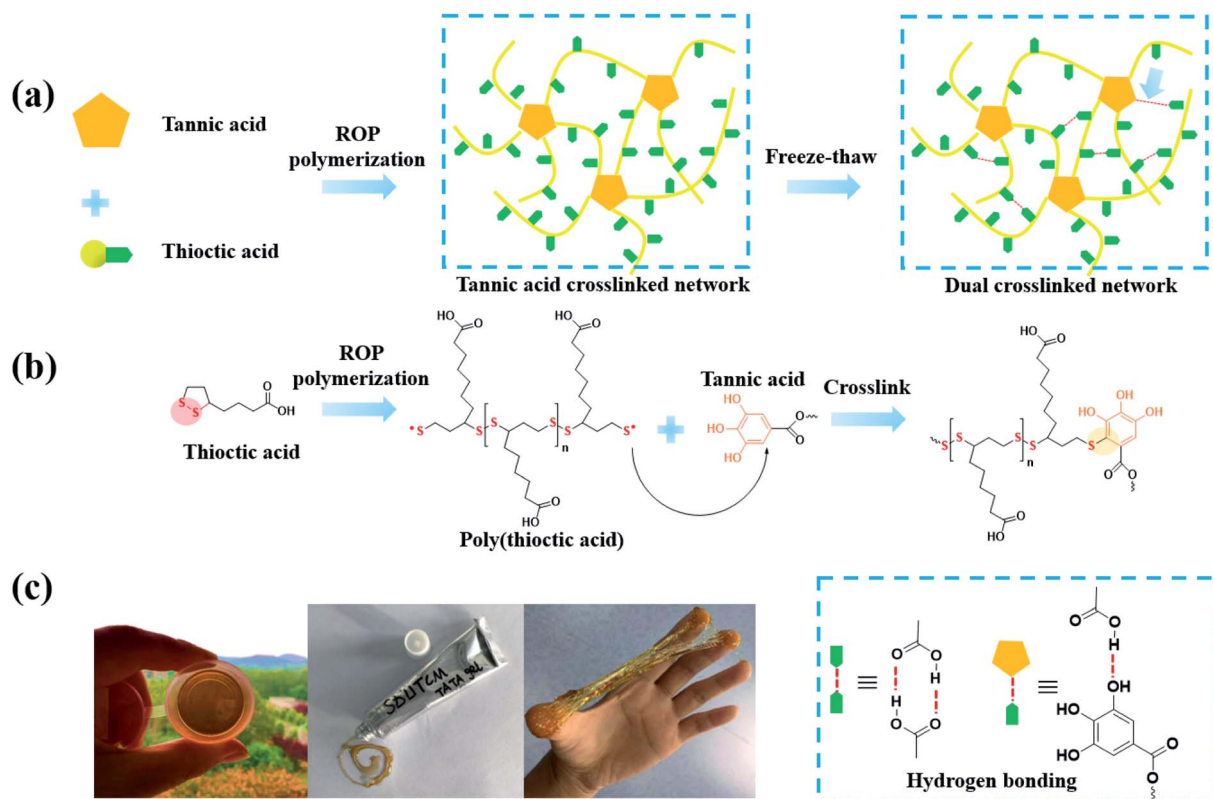
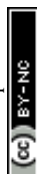


Fig. 14 (a) A schematic illustration of the synthetic route of TATA hydrogel; (b) Mechanism of the polyphenol-thiyl radical oxidation reaction; (c) photos of the TATA hydrogel. Reproduced from ref. 131 with permission from the Royal Society of Chemistry, copyright 2021.

Table 2 Applications of TA-crosslinked networks

Application	Composition	Crosslinking method	Ref.
Bone regeneration	TA-hydroxyapatite-collagen-peptide	Hydrogen bonding, MPN network and hydrophobic interaction	138
	TA-hydroxyapatite-silk fiber	Hydrogen bonding and MPN network	139
	TA-calcium alginate-peptide	Hydrogen bonding and MPN network	140
Skin adhesive for coagulation	TA-PVA-polyacrylamide	Hydrogen bonding	144
	TA-PAAm-kaolin	Hydrogen bonding, MPN network and radical oxidation	146
	TA-poly(glutamic acid)	Hydrogen bonding	147
Skin adhesive for UV resistance	TA-poly(thiocetic acid)	Hydrogen bonding and radical oxidation	131
Wound healing	TA-gelatin-gellan	Hydrogen bonding	152
	TA-PEG	Hydrogen bonding	153
	TA-hydroxypropyl chitin-Fe <sup>III</sup>	Hydrogen bonding and MPN network	154
Drug loading	TA-silk fiber-peptide	Hydrogen bonding and hydrophobic interaction	155
	TA-chitosan-silk fiber-Fe <sup>III</sup>	Hydrogen bonding and MPN network	156
	TA-indocyanine green-DOX	$\pi$ - $\pi$ interaction and electronic interaction	166
Photothermal material	TA-MSN-tetraethylenepentamine-DOX	Michael addition and Schiff base reaction	167
	TA-sericin-DOX-Fe <sup>III</sup>	MPN network	169
	TA-Fe <sup>III</sup> /V <sup>III</sup> /Ru <sup>III</sup>	MPN network	171
<i>In situ</i> generation of noble metal nanoparticles	TA-wood-Fe <sup>III</sup>	MPN network	174
	TA-graphene-Au <sup>III</sup>	$\pi$ - $\pi$ interaction and MPN network	53
	TA-graphene-Ag <sup>I</sup> -polyaspartamide	$\pi$ - $\pi$ interaction and MPN network	45
Antifouling coating	TA-PEG-Au <sup>III</sup> /Ag <sup>I</sup>	Mitsunobu reaction and MPN network	122
	TA-diethylenetriamine	Michael addition	80
	TA-thiol end-capped hyperbranched polyglycerols	Michael addition	94
	TA-glutaraldehyde- $\beta$ -FeOOH-1-dodecanethiol	Michael addition and phenol-aldehyde reaction	125



hydrogels, nanoparticles, injectable adhesives, coatings, microspheres and so on. Thanks to the flexible crosslinking method, tunable binding substrates and multifunctional properties of polyphenols, TA-based materials have recently been extensively applied in research areas such as bone regeneration, skin adhesives, wound dressings, drug loading and photothermal materials (Table 2). In this section, TA-crosslinked networks with multiple crosslinking strategies are introduced, which play a critical role in material performance.

#### 4.1. Bone regeneration

Nowadays, scaffolds aimed at the restoration of injured tissues have been reckoned to be the main topic in the field of tissue engineering applications.<sup>132</sup> Most musculoskeletal defects are caused by tumors, bone marrow diseases, external force, traffic accidents, battlefield injuries, and even bone birth defects, giving rise to degeneration of hyaline cartilage and subchondral bone.<sup>133</sup> To overcome these problems, conventional devices such as metallic plates and screws usually suffer from acute rejection, aseptic loosening, and a second operation for removal.<sup>134</sup> Though synthetic polymer-based 3D porous scaffolds including poly(methyl methacrylate) (PMMA) and calcium phosphate (CPC) bone cements have aroused more and more interest as alternative treatments, several drawbacks have emerged, such as low levels of osteogenesis, poor biocompatibility, and toxic degradation products as well as poor adhesion.<sup>135</sup> TA can be used as a bioactive component in fabricating a tissue engineering material with desirable antioxidant and anti-inflammatory properties. Thanks to its glue-like properties, including metal chelation, hydrogen bonds and  $\pi$ - $\pi$  stacking, TA can form networks with proteins, hydroxyapatite, and naturally derived reinforced polymers to form hierarchical microstructures with appropriate adhesion performance in a physiological environment.<sup>136,137</sup> Recently, multiple findings have suggested that TA is an effective surface modification intermediate and crosslinking aid in bone regeneration.

Based on the viewpoint that TA plays a role as a biocompatible multisite crosslinker for collagen as well as a growth-factor-delaying ingredient, Lee *et al.* designed new bone regeneration scaffolds composed of TA, calcium-deficient hydroxyapatite (CDHA), collagen, and plate-rich plasma (PRP) fabricated *via* a low-temperature printing process.<sup>138</sup> Controlled release of the

growth factors from this biocomposite was observed up to 35 days due to gradual degradation of the TA-based network. The cell proliferation and bone mineralization of this bone regeneration scaffold were substantially better than those without TA modification. Similar work on TA-hydroxyapatite composites was also exhibited by Bai *et al.*, in which phenolic chemistry was used as a robust synthetic protocol for fabricating a bone adhesive with low toxicity and high mechanical performance containing silk fibroin (SF), TA and hydroxyapatite (SF@TA@HA) (Fig. 15).<sup>139</sup> Typically, TA assembled with SF to form a nano-fibrillar structure with  $\beta$ -sheet-rich architecture, further strengthened by  $\text{Ca}^{2+}$ -phenolic coordination bridges. This composite accelerated the regeneration of bone defects at the initial stage *in vivo* with strong water-resistant fixation. Inspired by the phenomenon that TA could form additional coordinate bridges with calcium ions belonging to Ca-alginate (CA) nanoparticles,<sup>140</sup> Zhang *et al.* created a composite scaffold fabricated by prime-coating Ca-alginate hydrogel with TA followed by loading peptides that were beneficial for osteogenesis.<sup>141</sup> A TA prime-coating process significantly increased the stability and mechanical properties of the scaffold, facilitating the immobilization of peptides for continuous delivery with an ignorable effect on tissue bioactivity.

#### 4.2. Skin adhesive

A protein-rich surface such as skin contains abundant functional groups, such as amide bonds, thiols and amines, which facilitates polyphenol-based coating through Michael addition and hydrogen bonding. TA has been employed as a pivotal component for the design of multifunctional coatings and adhesive hydrogels for skin adhesion. Though the TA-based adhesives had a relatively low adhesive strength compared with PDA, they exhibited outstanding advantages in terms of low cost, biocompatibility, cell adherence and desirable drug loading capacity.<sup>142,143</sup> Moreover, owing to the polyphenol adhesion mechanism, TA-based adhesives exhibited water resistance and wet skin adhesion during practical uses, adapting to dynamic physiological conditions such as bleeding or leaching.<sup>144</sup>

TA-based adhesive hydrogels normally match the skin surface excellently with no skin sensitization or irritation. A combination between TA and a mechanical reinforcing agent

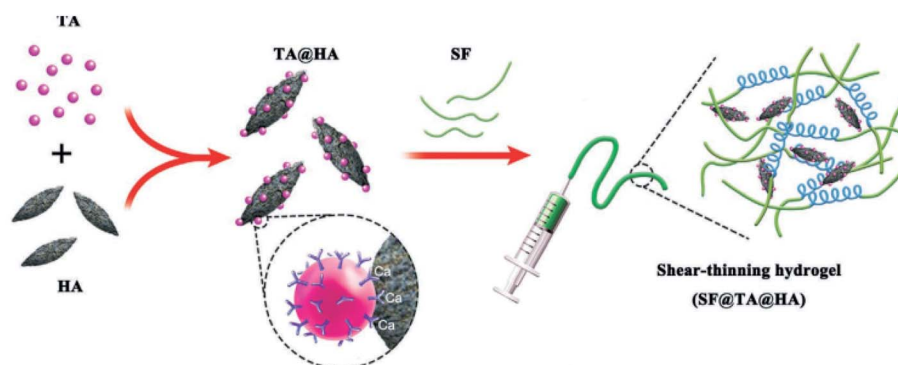


Fig. 15 TA-based adhesive hydrogel for bone regeneration. Reproduced from ref. 139 with permission from Wiley-VCH, copyright 2019.



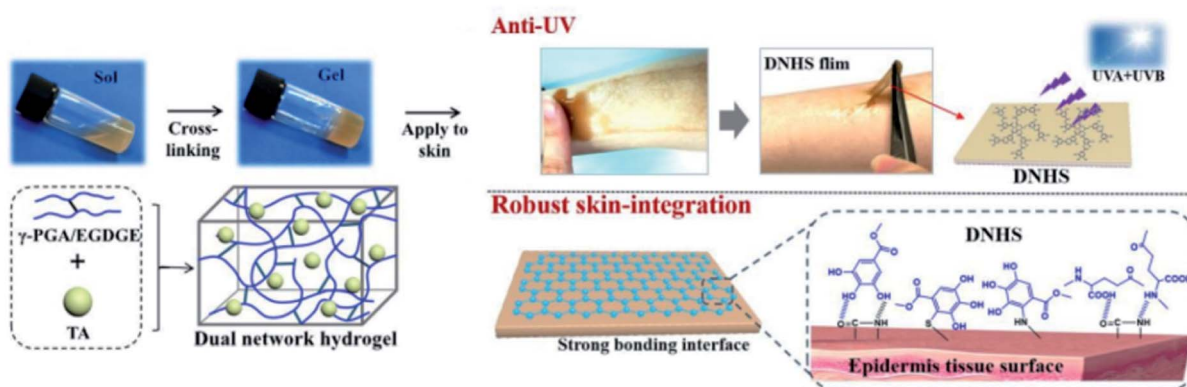


Fig. 16 Chemical crosslinking structure of a dual-network hydrogel sunscreen (DNHS) and its skin adhesion mechanism. Reproduced from ref. 147 with permission from the American Chemical Society, copyright 2019.

gives rise to a hybrid adhesive with excellent and repeatable adhesion to versatile substrates.<sup>145</sup> Based on this concept, Fan *et al.* developed a PAAm-TA-kaolin (KA) hydrogel for quick hemostatic application on bleeding skin.<sup>146</sup> In detail, TA served not only as a chemical crosslinker but also as a polyphenol donor for wet adhesion. Meanwhile, KA played roles as a physical crosslinker as well as a hemostatic accelerator. The dual-crosslinked PAAm-TA-KA hydrogel possessed high toughness and universal adhesiveness. The hemostatic time of this hydrogel on a rat femoral artery model was as short as 24 s in contrast to 148 s of the control group. Similar work on PAAm-TA complexes was provided by Fan *et al.*<sup>144</sup> Recently, a new dual-network hydrogel sunscreen (DNHS) based on poly- $\gamma$ -glutamic acid ( $\gamma$ -PGA) and TA was developed by Wang *et al.* (Fig. 16).<sup>147</sup> The driving force of gelation was induced by the intermolecular hydrogen bond between  $\gamma$ -PGA and TA, which endowed the hydrogel with remarkable self-recovery properties (within 60 s), excellent skin-integration, water resistance capacities and low peel strength. Considering the UV absorption characteristics of TA, this hydrogel demonstrated prominent UV skin protection performance across the broad UV region (360–275 nm).

#### 4.3. Antibacterial biomaterial for wound healing

The application of TA in wound healing can be traced back to the 1920s since TA-protection of lesion location from microbe or virus intrusion.<sup>148</sup> Since TA could interact with various biomacromolecules through supramolecular interactions, the antibacterial mechanism of TA is potentially associated with the cell wall complexation or membrane disruption initiated by oxidized TA.<sup>75</sup> Accompanied by the discovery of mussel-inspired coatings, there has come about a renewed viewpoint on the efficacy of TA as an adjuvant therapy for antibacterial wound dressings. Currently, other wound dressings including silk fibroin (SF), gellan, chitosan, hyaluronic acid (HA), collagen and alginate are also being developed for therapeutic treatment.<sup>149</sup> However, the use of toxic crosslinkers or organic solvents during the modification process poses an issue for long-term safety.<sup>150</sup> To meet diverse demands, such as adhesion ability, flexibility, physical or chemical tunability of wound dressings, it is reasonable to employ TA as a green crosslinker for

biomacromolecules or polymers, achieving multifunctionality and multitargeted uses.<sup>151</sup>

As for TA-based injectable hydrogels for wound healing, Zheng *et al.* verified that TA-loaded gellan hydrogel could accelerate wound healing in contrast to control groups.<sup>152</sup> Moreover, Sun *et al.* fabricated a self-healing injectable adhesive *via* a supramolecular interaction between TA and eight-armed PEG end-capped with succinimide glutarate active ester (PEG-SG) (Fig. 17).<sup>153</sup> Taking advantage of the hydrogen bonding induced by PEG segments and phenolic hydroxyl groups, as well as the ester exchange induced by succinimide and the tissue amino groups, this adhesive was capable of adhering to porcine tissues and sealing the rigid vascular artery. Ma *et al.* recently developed a thermal/pH responsive chitin/TA/ferric ion (HPCH/TA/Fe) composite hydrogel.<sup>154</sup> TA played roles not only as a crosslinker to improve mechanical properties, but also as an antibacterial agent sustainably released under acidic circumstances. The relevant examinations revealed that this hydrogel could efficiently resist wound infection while accelerating the healing process with appendage-filled and scarless skin.

Hydrogel patches or self-supporting 3D hydrogels are also recognized as an effective choice in clinical wound healing, especially those prepared from natural building blocks. For instance, the combination between TA and SF was constantly applied in superficial wound dressings. Jing *et al.* explored a TA-induced gelation method for SF *via* multiple interactions such as hydrogen bond association, hydrophobic interactions and  $\pi$ - $\pi$  interactions.<sup>155</sup> Acceleration of the wound healing process was observed by a full-thickness skin defect model on mice, revealing the fact that the incorporation of TA endowed the hydrogel with desirable bioactivity. Similar work was reported by Yu *et al.*<sup>156</sup> They designed a hybrid hydrogel composed of chitosan, silk fibroin, TA and ferric ions for photothermal therapy in wound healing. The spongy structure of the concerned hydrogel enable it to absorb large capacities of blood and tissue exudate, which was effective for bleeding wounds.

In particular, micro-biomedicine for wound healing is also attractive because of its extensive specific surface area, deep penetration and accurate quantification.<sup>157</sup> Instead of using toxic epichlorohydrin or polyphosphate as a crosslinker, TA can





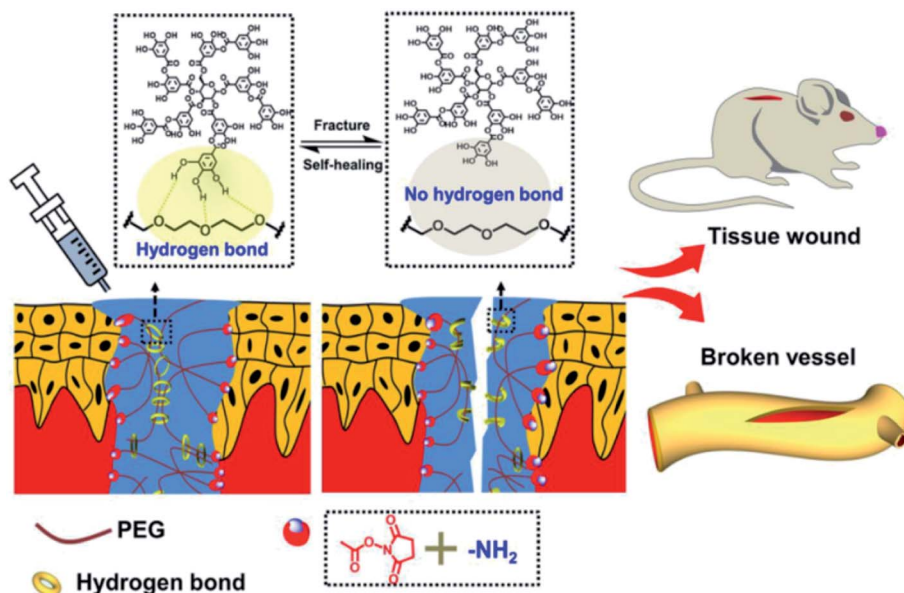


Fig. 17 Schematic exhibition of the PEG-SG/TA injectable hydrogel and its application in wound healing. Reproduced from ref. 153 with permission from the American Chemical Society, copyright 2020.

be used to stabilize HA microparticles for wound healing, as reported by Li *et al.*<sup>158</sup> This kind of hemostatic microparticle was promising in clinical applications because of its wide spectrum antibacterial activity against both *Escherichia coli* and *Staphylococcus aureus*. Notably, the wound can be repaired rapidly by TA-functionalized HA microspheres in 14 days.

#### 4.4. Drug loading vehicle

So far, cancer has always been one of the main threats to human health.<sup>159</sup> Chemotherapy combined with nanotechnology is the most frequently used solution with prolonged blood circulation time, enhanced safety and intracellular drug release.<sup>160–162</sup> TA was also involved in constructing smart, biodegradable, highly chemically tunable nanovehicles *via* multiple supramolecular interactions with payloads or other building units. As seen in Sections 2.1 and 2.3, TA-based polymer networks are generally

pH sensitive and have the ability to reconstruct under neutral or alkaline conditions, facilitating on-demand or controlled drug release *in vivo*.<sup>68</sup> Meanwhile, TA can promote the loading capacity of DOX *via*  $\pi$ - $\pi$  interactions and TA also provides reactive sites for binding a targeting ligand, which enhances therapeutic efficiency and lowers toxic side effects.<sup>163</sup>

Nowadays, considering the fact that the tumor site has a weakly acid microenvironment, pH-responsive release has become the most widely used application.<sup>164,165</sup> Deng *et al.* constructed a hybrid nano-transformer containing DOX, TA and indocyanine green, which was named DTIG. In this nano-material,  $\pi$ - $\pi$  interactions and electronic interactions were the driving force for self-assembly (Fig. 18a).<sup>166</sup> In this DTIG system, TA significantly reduced the nonspecific binding of nanovehicles, realized controlled release in blood circulation and avoided phagocytosis of the reticuloendothelial system (RES). In

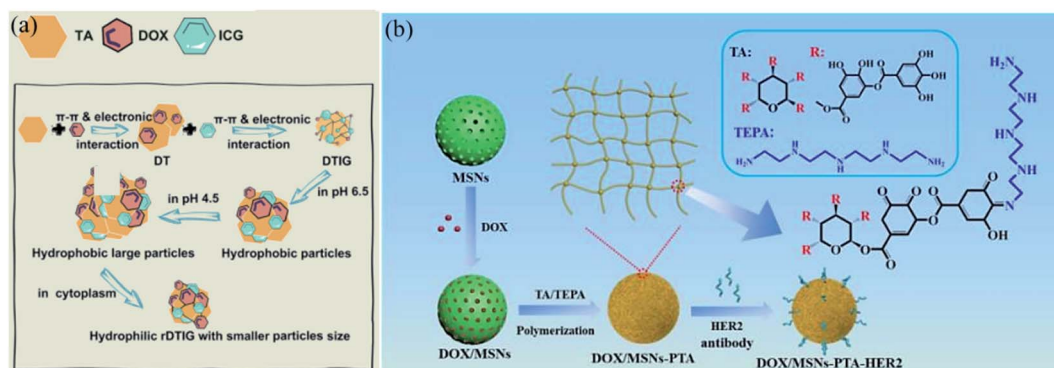


Fig. 18 (a) The construction of a TA-based nanotransformer (DTIG) and its controlled release under acidic environments. Reproduced from ref. 166 with permission from the American Chemical Society, copyright 2020. (b) Drug delivery process of TA-coated MSNs for accurate cancer treatment. Reproduced from ref. 167 with permission from the Royal Society of Chemistry, copyright 2020.

the lysosomal environment (pH 4.5), DTIG reassembled into a giant nanoreassembly (1.5  $\mu\text{m}$ ) in association with a hydrophobic-hydrophilic conversion, which gave rise to rapid lysosome escape and accurate intracellular payload release. Chen *et al.* also created a pH-responsive drug delivery system by applying TA as a “gatekeeper”.<sup>167</sup> In brief, TA and tetraethylenepentamine (TEPA) were polymerized through a Schiff-base/Michael addition reaction to form a pH-sensitive shell, which was coated on the surface of mesoporous silica nanoparticles (MSNs) (Fig. 18b). The TA-TEPA binary coating shell could dissociate into a loose state under acidic conditions for drug release. When the surroundings returned to alkaline or neutral, the TA-TEPA shell reassembled again to stop drug discharge. Additionally, TA/ferric ion ( $\text{Fe}^{3+}$ ) MPN capsules were also applied in smart, pH-dependent drug delivery for cancer cells, as reported by Zhu *et al.*<sup>168</sup> and Liu *et al.*,<sup>169</sup> which effectively prevent premature drug leakage in healthy tissues while unloading payloads in feedback to the acidic tumor and intracellular-microenvironments.

#### 4.5. Photothermal material

TA-based MPN networks for seawater desalination, cancer therapy, solar harvesting and near infra-red (NIR) light-induced actuation have aroused wide interest due to their high stability, facile synthetic procedure, biosafety, biocompatibility and high photothermal conversion rate.<sup>170,171</sup> Moreover, MPNs can effectively adsorb various aromatic molecules, ready for versatile chemical modifications.<sup>172</sup> Researchers have proved that the photothermal conversion mechanism lay in the ligand-to-metal

charge transfer between multivalent metal ions and TA.<sup>173</sup> Wang *et al.* confirmed that  $\text{Fe}^{\text{III}}$ -TA complexes achieved the highest NIR absorbance in contrast to other nitrophenols, including gallic acid, pyrogallol and epigallocatechin gallate (EGCG), probably because TA possessed more vicinal diol groups and had a better chance of coming into contact with  $\text{Fe}^{\text{III}}$ .<sup>174</sup>

Numerous studies stated that the TA/ $\text{Fe}^{\text{III}}$  complex was promising in the desalination of seawater. Recently, He *et al.* proposed a simple, mild and versatile method for preparing photothermal wood toward solar steam generation (Fig. 19).<sup>175</sup> They found that TA and  $\text{Fe}^{3+}$  can effectively transform different kind of wood into photothermal material (wood-TA- $\text{Fe}^{\text{III}}$ ), which could be realized in aqueous phase at room temperature without any high-cost metals. Such wood exhibits outstanding thermal performance, such as corrosion-resistance, long-term anti-rinsing and durable service. Similar work could be seen in the work undertaken by Wang *et al.* using a TA/PVP/ $\text{Fe}^{\text{III}}$  complex coated onto a polyurethane sponge.<sup>176</sup> Recent progress on photothermal therapy for tumors was shown by Shi *et al.*,<sup>177</sup> in which a TA/ $\text{Fe}^{\text{III}}$  complex coated mesoporous silica nanoparticle (MSN-pTA) was designed. Under 808 nm laser irradiation, dissociation of the TA/ $\text{Fe}^{\text{III}}$  complex occurred and the loaded DOX inside MSN was released, achieving combined chemo-photothermal therapy. Chen *et al.* constructed TA-hybridized mixed valence vanadium oxide nanosheets (TA@VO<sub>x</sub> NSs), which possessed excellent NIR-light mediated conversion ability to inhibit tumors.<sup>178</sup> In the case of solar harvesting, Huang *et al.* combined TA with liquid metals to realize photothermal materials with high efficiency, which

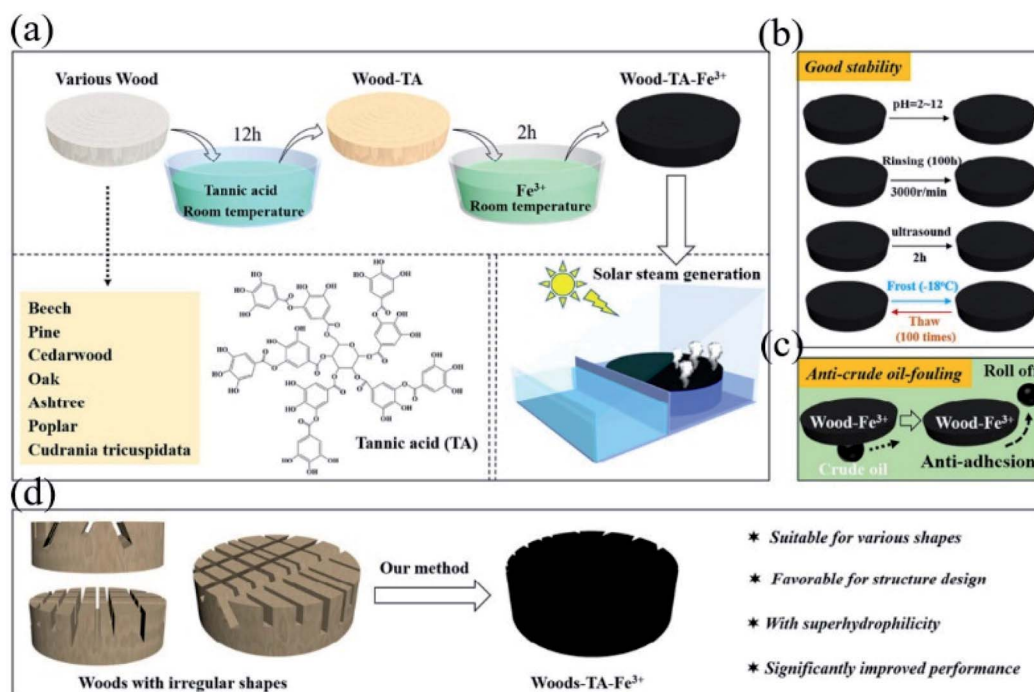


Fig. 19 (a) Wood modified by an MPN network for solar steam generation; (b) wood with excellent corrosion-resistance; (c) anti-crude oil-fouling character of the resultant MPN-based photothermal materials; (d) exclusive advantages of the methods for enlarging the specific surface area of wood. Reproduced from ref. 175 with permission from Elsevier, copyright 2020.



manifested strong broad-band light absorption (96.9–99.3%) and excellent photothermal conversion ability ( $\eta_{PT} = 77.3\%$ ).<sup>179</sup> In particular, TA-based MPN networks could also be utilized in (NIR) light-triggered actuation. As proposed by Wang *et al.*,<sup>180</sup> a TA/WS<sub>2</sub>/polyurethane latex was coated onto a cellulose nanofiber film to form a bi-layer flexible device. Since the photothermal conversion performance of TA/WS<sub>2</sub>/polyurethane latex was more excellent than that of cellulose nanofiber film, the NIR-induced actuation could be realized based on the mismatch of thermal expansion between the two layers.

## 5. Conclusions and future prospects

This review has systematically summarized various protocols leading to tannic-acid-based materials with a wide scope of functions and applications. The underlying reason why tannic acid is prevalent for building versatile polymeric networks lies in the multi-pyrogallol moieties as reactive binding sites. According to various natural inspirations as well as research findings, tannic acid has previously been used as a crosslinking agent with proteins, polysaccharides, hydrogen bonding acceptors, polycations, metal ions and other functional molecules. In view of physical crosslinking, tannic acid could achieve supramolecular materials such as hydrogels, reductive graphene complexes and nanocapsules through hydrogen bonding,  $\pi$ - $\pi$  stacking and metal-polyphenol interactions. Covalent bonding through chemical crosslinking enhanced the stability of the resulting poly(tannic acid). Molecules bearing amine, thiol, epoxy, boronate, alcoholic hydroxyl, anhydride, carboxyl moieties and thiyl radicals are capable of reacting with a polyphenol group whether in a Michael addition or in nucleophilic ways. Moreover, tannic acid is recognized as a low-cost dopamine analogue owing to its abundant natural resources, rapid deposition property and nontoxicity, which is promising in developing new functional materials through scale-up productions. Though other forms polyphenols, such as epigallocatechin-3-gallate, proanthocyanidins, caffeic acid, resveratrol and so on have received a lot of attention, they could not be used instead of tannic acid because of their high cost, low chemical stability and limited binding sites. Possessing biocompatibility, antimicrobial properties, smart self-assembly capability and reductive ability, tannic acid has aroused more and more attention in the fields of macromolecular biomaterials. Incorporating the special properties of tannic acid and other building blocks, a wide range applications of tannic-acid-crosslinked networks, including bone regeneration, skin adhesives, wound dressings, drug loading vehicles and photothermal materials, have been studied by numerous researchers recently. In future prospects, tannic acid also shows potential in combination with other new materials at the frontier of science, such as black phosphorus, MXene, and graphyne, to achieve wider fields of application.

The initial tannic-acid-crosslinked materials were mainly metal-phenol networks with various nanostructures. Over time, macroscopic three-dimensional materials containing tannic acid, especially adhesive hydrogels, have been developed in numerous studies, in which researchers found that hydrophilic

polymeric substrates are necessary for constructing a long-range, highly hydrated network. The latest trends for a tannic-acid-based network could be summarized as follows: (i) new crosslinking methods have emerged, including phenol-alcohol reactions, acylation of polyphenols, polyphenol-thiyl radical oxidation reaction, silanol-phenol and phenol-epoxy ring-opening reaction. (ii) In practical applications, tannic-acid-crosslinked biomacromolecules, such as silk fibers, gelation, gellan, peptides and polysaccharides, have received widespread interest owing to their biocompatibility, biodegradability, adhesiveness, and mechanical reinforcement, as well as facile preparation. (iii) A combination of multiple crosslinking methods has become more and more common, which is beneficial for integrating the advantages of various raw materials. (iv) A macroscopic combination between tannic-acid-based materials and other flexible materials has been studied, in which a tannic-acid-based complex was used as a coating or a functional layer to form smart devices. (v) Besides the anti-microbial, antioxidant and anti-inflammatory properties of tannic acid, researchers have exploited other properties, such as UV adsorption, photothermal conversion and chemodynamic responsiveness. Above all the latest trends, a hybrid material that incorporates new substrates is the main theme of progress on tannic-acid-crosslinked networks.

However, challenges still exist and advances in this field are demanded. Firstly, the coacervation between tannic acid and polymers owing to rapid multisite binding has become an obstacle for developing new complexes with even better performance, which requires an accurate feeding ratio and pH regulation. Though basic conditions could resist the formation of coacervation, the oxidation progress of tannic acid could not be ignored. Secondly, tannic acid tends to bind randomly to hydrogen bonding acceptors, leading to an amorphous rather than long-range-ordered material with weak mechanical strength. In other words, a conjugated multidentate ligand with high molecular weight for tannic acid could further expand this research area in organic-organic frameworks, organic-inorganic hybrid frameworks and directionally solidified materials. Thirdly, other than synthetic polymer-tannic acid conjugates, the exact binding mechanism of polysaccharide-tannic acid conjugates has yet to be more thoroughly studied, considering the fact that there are numerous forms of polysaccharides in nature, which limits the utilization of polysaccharide-tannic acid in the preparation of hydrogels, 3D printing inks and organic films. Last but not least, the reaction between polyphenol and radicals features rapid kinetics and robust preparation, which provides a horizon for new functional networks. Therefore, further efforts on synthetic procedures, post-functional methods and the accurate design of building blocks leading to a TA-based network will continue to be of great interest.

Overall, in the past few decades, mussel-inspired catechol chemistry has added new life and vigor to tannic acid in building various polymeric complexes. In view of the rising severe environmental problems derived from the unsustainable petrochemical industry, tannic-acid-crosslinked functional polymeric networks provide a green platform with a facile,





sustainable, wide source and abundant content manner. Although many mechanisms concerning the association and disassembly of tannic-acid-based materials still remain unclear or controversial, abundant research on tannic-acid-crosslinked functional polymeric networks has emerged recently, showing that this field is gradually deepening and expanding. It could be inferred that tannic-acid-based functional materials will continue to be of great interest for researchers, especially in biomedicine, nano-technology, catalysis and energy storage.

## Conflicts of interest

There are no conflicts to declare.

## Acknowledgements

The study was supported by the Health Commission of Shandong Province (Grant No. 202004010938).

## References

- J. L. Guo, Y. Ping, H. Ejima, K. Alt, M. Meissner, J. J. Richardson, Y. Yan, K. Peter, D. v. Elverfeldt, C. E. Hagemeyer and F. Caruso, *Angew. Chem., Int. Ed.*, 2014, **53**, 1–7.
- Y. L. Liu, K. L. Ai and L. H. Lu, *Chem. Rev.*, 2014, **114**, 5057–5115.
- Z. Nie, A. Petukhova and E. Kumacheva, *Nat. Nanotechnol.*, 2010, **5**, 15–25.
- L. Xu, W. Ma, L. Wang, C. Xu, H. Kuang and N. A. Kotov, *Chem. Soc. Rev.*, 2013, **42**, 3114–3126.
- E. Munch, M. E. Launey, D. H. Alsem, E. Saiz, A. P. Tomsia and R. O. Ritchie, *Science*, 2008, **322**, 1516–1520.
- T. S. Sileika, D. G. Barrett, R. Zhang, K. H. A. Lau and P. B. Messersmith, *Angew. Chem., Int. Ed.*, 2013, **52**, 10766–10770.
- S. Quideau, D. Deffieux, C. Douat-Casassus and L. Pouysegu, *Angew. Chem., Int. Ed.*, 2011, **50**, 586–621.
- B. N. Singh, S. Shankar and R. K. Srivastava, *Biochem. Pharmacol.*, 2011, **82**, 1807–1821.
- H. Ejima, J. J. Richardson and F. Caruso, *Polym. J.*, 2014, **46**, 452–459.
- A. King and G. Young, *J. Am. Diet. Assoc.*, 1999, **99**, 213–218.
- S. Zhao, S. C. Xie, X. L. Liu, X. M. Shao, Z. Zhao, Z. X. Xin and L. Li, *J. Polym. Res.*, 2018, **25**, 225.
- S. Z. Moghaddam, S. Sabury and F. Sharif, *RSC Adv.*, 2014, **4**, 8711–8719.
- C. Zhu, E. Chalmers, L. M. Chen, Y. Q. Wang, B. B. Xu, Y. Li and X. Q. Liu, *Small*, 2019, **15**, 1902440.
- Z. Wang, S. Zhao, R. Song, W. Zhang, S. Zhang and J. Li, *Sci. Rep.*, 2017, **7**, 9664.
- A. E. Hagerman, K. M. Riedl, G. A. Jones, K. N. Sovik, N. T. Ritchard, P. W. Hartzfeld and T. L. Riechel, *J. Agric. Food Chem.*, 1998, **46**, 1887–1892.
- Y. Du, W. Z. Qiu, Z. L. Wu, P. F. Ren, Q. Zheng and Z. K. Xu, *Adv. Mater.*, 2016, **3**, 1600167.
- T. Yoshida, T. C. Lai, G. S. Kwon and K. Sako, *Expert Opin. Drug Delivery*, 2013, **10**, 1497–1513.
- F. Jehle, P. Fratzl and M. J. Harrington, *ACS Nano*, 2018, **12**, 2160–2168.
- U. T. Khatoon, G. N. Rao, M. K. Mohan, A. Ramanaviciene and A. Ramanavicius, *J. Environ. Chem. Eng.*, 2018, **6**, 5837–5844.
- X. Huang, H. Wu, X. Liao and B. Shi, *Green Chem.*, 2010, **12**, 395–399.
- A. Sionkowska, B. Kaczmarek, M. Gnatowska and J. Kowalonek, *J. Photochem. Photobiol., B*, 2015, **148**, 333–339.
- V. Kozlovskaya, O. Zavgorodnya, Y. Chen, K. Ellis, H. M. Tse, W. Cui, J. A. Thompson and E. Kharlampieva, *Adv. Funct. Mater.*, 2012, **22**, 3389–3398.
- S. Zhao, S. C. Xie, Z. Zhao, J. L. Zhang, L. Li and Z. X. Xin, *ACS Sustainable Chem. Eng.*, 2018, **6**, 7652–7661.
- J. Fu, Z. Chen, M. Wang, S. Liu, J. Zhang, J. Zhang, R. Han and Q. Xu, *Chem. Eng. J.*, 2015, **259**, 53–61.
- R. G. Andrade, L. T. Dalvi, J. M. C. Silva, G. K. B. Lopes, A. Alonso and M. Hermes-Lima, *Arch. Biochem. Biophys.*, 2005, **437**, 1–9.
- D. E. Payne, N. R. Martin, K. R. Parzych, A. H. Rickard, A. Underwood and B. R. Boles, *Infect. Immun.*, 2013, **81**, 496–504.
- J. Luo, J. Lai, N. Zhang, Y. Liu, R. Liu and X. Liu, *ACS Sustainable Chem. Eng.*, 2016, **4**, 1404–1413.
- W. Chou, Y. Wang, K. Chen, J. Wu, C. Liang and S. H. Juo, *Cell. Immunol.*, 2012, **273**, 79–84.
- I. Erel-Unal and S. A. Sukhishvili, *Macromolecules*, 2008, **41**, 3962–3970.
- F. Reitzer, M. Allais, V. Ball and F. Meyer, *Adv. Colloid Interface Sci.*, 2018, **257**, 31–41.
- S. Hong, J. Yeom, I. T. Song, S. M. Kang, H. Lee and H. Lee, *Adv. Mater. Interfaces*, 2014, **1**, 1400113.
- S. M. Burkinshaw and N. Kumar, *Dyes Pigm.*, 2009, **80**, 53–60.
- Y. Lei, Z. Tang, R. Liao and B. Guo, *Green Chem.*, 2011, **13**, 1655–1658.
- M. Cencer, M. Murley, Y. Liu and B. P. Lee, *Biomacromolecules*, 2015, **16**, 404–410.
- V. Natarajan, N. Krithica, B. Madhan and P. K. Sehgal, *J. Biomed. Mater. Res., Part B*, 2013, **101**, 560–567.
- C. Zhang, B. H. Wu, Y. S. Zhou, F. Zhou, W. M. Liu and Z. K. Wang, *Chem. Soc. Rev.*, 2020, **49**, 3605–3637.
- J. Saiz-Poseu, J. Mancebo-Aracil, F. Nador, F. Busqué and D. Ruiz-Molina, *Angew. Chem., Int. Ed.*, 2019, **58**, 696–714.
- M. Rinaudo, B. Lardy, L. Grange and T. Conrozier, *Polymers*, 2014, **6**, 1948–1957.
- T. Shutava, M. Prouty, D. Kommireddy and Y. Lvov, *Macromolecules*, 2005, **38**, 2850–2858.
- K. H. Hong, *Polym. Bull.*, 2017, **74**, 2861–2872.
- W. W. Niu, Y. L. Zhu, R. Wang, Z. Y. Lu, X. K. Liu and J. Q. Sun, *ACS Appl. Mater. Interfaces*, 2020, **12**, 30805–30814.
- H. Y. Lee, C. H. Hwang, H. E. Kim and S. H. Jeong, *Carbohydr. Polym.*, 2018, **186**, 290–298.





- 43 X. C. Du, L. Wu, H. Y. Yan, L. J. Qu, L. N. Wang, X. Wang, S. Ren, D. L. Kong and L. Y. Wang, *ACS Biomater. Sci. Eng.*, 2019, **5**, 2610–2620.
- 44 C. Y. Liu, H. Y. Liu, K. Y. Tang, K. K. Zhang, Z. X. Zou and X. P. Gao, *J. Polym. Environ.*, 2020, **28**, 984–994.
- 45 B. Wang, J. R. Moon, S. Ryu, K. D. Park and J. H. Kim, *Polym. Compos.*, 2020, **41**, 2578–2587.
- 46 N. Srivastava, M. Srivastava, V. K. Gupta, P. Ramteke and P. Mishra, *Bioresour. Technol.*, 2018, **270**, 337–345.
- 47 R. K. Layek, K. R. Ramakrishnan, E. Sarlin, O. Orell, M. Kanerva, J. Vuorinen and M. Honkanen, *J. Mater. Chem. A*, 2018, **6**, 13203–13214.
- 48 J. Luo, N. Zhang, R. Liu and X. Liu, *RSC Adv.*, 2014, **4**, 64816–64824.
- 49 K. Liu, H. Li, Y. Wang, X. Gou and Y. Duan, *Colloids Surf., A*, 2015, **477**, 35–41.
- 50 J. Wang, Z. Shi, J. Fan, Y. Ge, J. Yin and G. Hu, *J. Mater. Chem.*, 2012, **22**, 22459–22466.
- 51 Z. Zhao, L. Li, X. M. Shao, X. L. Liu, S. Zhao, S. C. Xie and Z. X. Xin, *Polym. Test.*, 2018, **70**, 396–402.
- 52 S. Zhao, S. C. Xie, P. P. Sun, Z. Zhao, L. Li, X. M. Shao, X. L. Liu and Z. X. Xin, *RSC Adv.*, 2018, **8**, 17813–17825.
- 53 J. Luo, N. Zhang, J. P. Lai, R. Liu and X. Y. Liu, *J. Hazard. Mater.*, 2015, **300**, 615–623.
- 54 P. He, J. Y. Wu, X. F. Pan, L. H. Chen, K. Liu, H. L. Gao, H. Wu, S. L. Cao, L. L. Huang and Y. H. Ni, *J. Mater. Chem. A*, 2020, **8**, 3109–3118.
- 55 K. Tan, R. Liu, J. Luo, Y. Zhu, W. Wei and X. Y. Liu, *Prog. Org. Coat.*, 2019, **130**, 214–220.
- 56 A. Bétard and R. A. Fischer, *Chem. Rev.*, 2012, **112**, 1055–1083.
- 57 L. Y. Chou, K. Zagorovsky and W. C. Chan, *Nat. Nanotechnol.*, 2014, **9**, 148–155.
- 58 R. Hayward, D. Saville and I. Aksay, *Nature*, 2000, **404**, 56–59.
- 59 M. P. Cecchini, V. A. Turek, J. Paget, A. A. Kornyshev and J. B. Edel, *Nat. Mater.*, 2013, **12**, 165–171.
- 60 S. J. Yang, M. Antonietti and N. Fechner, *J. Am. Chem. Soc.*, 2015, **137**, 8269–8273.
- 61 A. Magasinski, P. Dixon, B. Hertzberg, A. Kvit, J. Ayala and G. Yushin, *Nat. Mater.*, 2010, **9**, 353–358.
- 62 S. Guo and S. Sun, *J. Am. Chem. Soc.*, 2012, **134**, 2492–2495.
- 63 T. K. Ross and R. A. Francis, *Corros. Sci.*, 1978, **18**, 351–361.
- 64 J. L. Guo, B. L. Tardy, A. J. Christofferson, Y. L. Dai, J. J. Richardson, W. Zhu, M. Hu, Y. Ju, J. W. Cui, R. R. Dagastine, I. Yarovsky and F. Caruso, *Nat. Nanotechnol.*, 2016, **11**, 1105–1111.
- 65 J. Lee, O. K. Farha, J. Roberts, K. A. Scheidt, S. T. Nguyen and J. T. Hupp, *Chem. Soc. Rev.*, 2009, **38**, 1450–1459.
- 66 Y. Gossuin, P. Gillis, A. Hocq, Q. L. Vuong and A. Roch, *Wiley Interdiscip. Rev.: Nanomed. Nanobiotechnol.*, 2009, **1**, 299–310.
- 67 Z. Peng and H. Zhong, *J. Macromol. Sci., Part B: Phys.*, 2014, **53**, 233–242.
- 68 H. L. Fan, L. Wang, X. D. Feng, Y. Z. Bu, D. C. Wu and Z. X. Jin, *Macromolecules*, 2017, **50**, 666–676.
- 69 N. Ninan, A. Forget, V. P. Shastri, N. H. Voelcker and A. Blencowe, *ACS Appl. Mater. Interfaces*, 2016, **8**, 28511–28521.
- 70 H. Li, X. X. Shu, P. R. Tong, J. H. Zhang, P. F. An, Z. X. Lv, H. Tian, J. T. Zhang and H. B. Xia, *Small*, 2021, **17**, 2102002.
- 71 T. T. Li, X. M. Hu, Q. S. Zhang, Y. Y. Zhao, P. Wang, X. Wang, B. T. Qin and W. Lu, *Polym. Adv. Technol.*, 2020, **31**, 1648–1660.
- 72 H. Lee, S. M. Dellatore, W. M. Miller and P. B. Messersmith, *Science*, 2007, **318**, 426–430.
- 73 X. Ao, Y. Wang, P. Jiang, S. Li and X. Huang, *Compos. Sci. Technol.*, 2018, **154**, 154–164.
- 74 M. A. North, C. A. D. Grosso and J. J. Wilker, *ACS Appl. Mater. Interfaces*, 2017, **9**, 7866–7872.
- 75 W. Zhang, R. X. Wang, Z. M. Sun, X. W. Zhu, Q. Zhao, T. F. Zhang, A. Cholewinski, F. K. Yang, B. X. Zhao, R. Pinnaratip, P. K. Forooshani and B. P. Lee, *Chem. Soc. Rev.*, 2020, **49**, 433–464.
- 76 W. Z. Qiu, G. P. Wu and Z. K. Xu, *ACS Appl. Mater. Interfaces*, 2018, **10**, 5902–5908.
- 77 B. Liu, B. Lyle and K. Thomas, *J. Am. Chem. Soc.*, 2006, **128**, 15228–15235.
- 78 J. Yang, M. A. Cohen Stuart and M. Kamperman, *ChemInform*, 2014, **43**, 8271–8298.
- 79 Y. Cao, N. Liu, W. Zhang, L. Feng and Y. Wei, *ACS Appl. Mater. Interfaces*, 2016, **8**, 3333–3339.
- 80 X. Zhang, Y. Lv, H. C. Yang, Y. Du and Z. K. Xu, *ACS Appl. Mater. Interfaces*, 2016, **8**, 32512–32519.
- 81 Q. Huang, J. Zhao, M. Y. Liu, J. Y. Chen, X. L. Zhu, T. Wu, J. W. Tian, Y. Q. Wen, X. Y. Zhang and Y. Wei, *J. Taiwan Inst. Chem. Eng.*, 2018, **82**, 92–101.
- 82 X. Zhang, M. D. Do, P. Casey, A. Sulistio, G. G. Qiao, L. Lundin, P. Lillford and S. Kosaraju, *J. Agric. Food Chem.*, 2010, **58**, 6809–6815.
- 83 H. W. Pang, S. J. Zhao, L. T. Mo, Z. Wang, W. Zhang, A. Huang, S. F. Zhang and J. Z. Li, *J. Appl. Polym. Sci.*, 2020, **137**, 48785.
- 84 S. J. Ge, N. Ji, S. N. Cui, W. Xie, M. Li, Y. Li, L. Xiong and Q. J. Sun, *J. Agric. Food Chem.*, 2019, **67**, 11489–11497.
- 85 J. S. Guo, W. Sun, J. P. Kim, X. L. Lu, Q. Y. Li, M. Lin, O. Mrowczynski, E. B. Rizk, J. G. Cheng, G. Y. Qian and J. Yang, *Acta Biomater.*, 2018, **72**, 35–44.
- 86 Q. X. Zhao, S. D. Mu, Y. R. Long, J. Zhou, W. Y. Chen, D. Astruc, C. Gaidau and H. B. Gu, *Macromol. Mater. Eng.*, 2019, **304**, 1800664.
- 87 Q. Lin, D. Gourdon, C. J. Sun, N. Holten-Andersen, T. H. Anderson, J. H. Waite and J. N. Israelachvili, *Proc. Natl. Acad. Sci. U. S. A.*, 2007, **104**, 3782–3786.
- 88 J. J. Wu, L. Zhang, Y. X. Wang, Y. H. Long, H. Gao, X. L. Zhang, N. Zhao, Y. L. Cai and J. Xu, *Langmuir*, 2011, **27**, 13684–13691.
- 89 H. Lee, N. F. Scherer and P. B. Messersmith, *Proc. Natl. Acad. Sci. U. S. A.*, 2006, **103**, 12999–13003.
- 90 L. Q. Xu, W. J. Yang, K. G. Neoh, E. T. Kang and G. D. Fu, *Macromolecules*, 2010, **43**, 8336–8339.
- 91 H. B. Zeng, D. S. Hwang, J. N. Israelachvili and J. H. Waite, *Proc. Natl. Acad. Sci. U. S. A.*, 2010, **107**, 12850–12853.



- 92 J. Imbrogno, M. D. Williams and G. Belfort, *ACS Appl. Mater. Interfaces*, 2015, **7**, 2385–2392.
- 93 X. F. Huang, J. W. Jia, Z. K. Wang and Q. L. Hu, *Chin. J. Polym. Sci.*, 2015, **33**, 284–290.
- 94 D. Pranantyo, L. Q. Xu, K. G. Neoh and E. T. Kang, *Ind. Eng. Chem. Res.*, 2016, **55**, 1890–1901.
- 95 L. Q. Xu, D. Pranantyo, K. G. Neoh, E. T. Kang and G. D. Fu, *ACS Sustainable Chem. Eng.*, 2016, **4**, 4264–4272.
- 96 R. Liu, J. J. Zhu, J. Luo and X. Y. Liu, *Prog. Org. Coat.*, 2014, **77**, 30–37.
- 97 J. F. Wu, S. Fernando, D. Weerasinghe, Z. G. Chen and D. C. Webster, *ChemSusChem*, 2011, **4**, 1135–1142.
- 98 M. Korey, G. P. Mendis, J. P. Youngblood and J. A. Howarter, *J. Polym. Sci., Part A: Polym. Chem.*, 2018, **56**, 1468–1480.
- 99 M. Qi, Y. J. Xu, W. H. Rao, X. Luo, L. Chen and Y. Z. Wang, *RSC Adv.*, 2018, **8**, 26948–26958.
- 100 X. M. Fei, W. Wei, F. Q. Zhao, Y. Zhu, J. Luo, M. Q. Chen and X. Y. Liu, *ACS Sustainable Chem. Eng.*, 2017, **5**, 596–603.
- 101 G. M. Roudsari, A. K. Mohanty and M. Misra, *ACS Sustainable Chem. Eng.*, 2014, **2**, 2111–2116.
- 102 Y. O. Kim, J. Cho, H. Yeo, B. W. Lee, B. J. Moon, Y. M. Ha, Y. R. Jo and Y. C. Jung, *ACS Sustainable Chem. Eng.*, 2019, **7**, 3858–3865.
- 103 X. M. Feng, J. Z. Fan, A. Li and G. Q. Li, *ACS Sustainable Chem. Eng.*, 2020, **8**, 874–883.
- 104 J. Handique, J. Gogoi, J. Nath and S. K. Dolui, *Polym. Eng. Sci.*, 2020, **60**, 140–150.
- 105 P. Baruah, R. Duarah and N. Karak, *Iran. Polym. J.*, 2016, **25**, 849–861.
- 106 W. Z. Qiu, H. C. Yang and Z. K. Xu, *Adv. Colloid Interface Sci.*, 2018, **256**, 111–125.
- 107 R. Sa, Y. Yan, Z. H. Wei, L. Q. Zhang, W. C. Wang and M. Tian, *ACS Appl. Mater. Interfaces*, 2014, **6**, 21730–21738.
- 108 Y. He, C. L. Chen, G. Q. Xiao, F. Zhong, Y. Q. Wu and Z. He, *React. Funct. Polym.*, 2019, **137**, 104–115.
- 109 C. Chen, X. Yang, S. J. Li, F. J. Ma, X. Yan, Y. N. Ma, Y. X. Ma, Q. H. Ma, S. Z. Gao and X. J. Huang, *RSC Adv.*, 2021, **11**, 5182–5191.
- 110 M. C. Roberts, M. C. Hanson, A. P. Massey, E. A. Karren and P. F. Kiser, *Adv. Mater.*, 2007, **19**, 2503–2507.
- 111 L. He, D. E. Fullenkamp, J. G. Rivera and P. B. Messersmith, *Chem. Commun.*, 2011, **47**, 7497–7499.
- 112 J. A. Burdick and W. L. Murphy, *Nat. Commun.*, 2012, **3**, 1269.
- 113 S. H. Hong, S. Kim, J. P. Park, M. Shin, K. Kim, J. H. Ryu and H. Lee, *Biomacromolecules*, 2018, **19**, 2053–2061.
- 114 J. N. Cambre and B. S. Sumerlin, *Polymer*, 2011, **52**, 4631–4643.
- 115 E. Faure, C. Falentin-Daudré, C. Jérôme, J. Lyskawa, D. Fournier, P. Woisel and C. Detrembleur, *Prog. Polym. Sci.*, 2013, **38**, 236–270.
- 116 B. M. W. Wohl and J. F. J. Engbersen, *J. Controlled Release*, 2012, **158**, 2–14.
- 117 U. Manna and S. Patil, *ACS Appl. Mater. Interfaces*, 2010, **2**, 1521–1527.
- 118 J. L. Guo, H. L. Sun, K. Alt, B. L. Tardy, J. J. Richardson, T. Suma, H. Ejima, J. W. Cui, C. E. Hagemeyer and F. Caruso, *Adv. Healthcare Mater.*, 2015, **4**, 1796–1801.
- 119 Z. J. Huang, P. Delparastan, P. Burch, J. Cheng, Y. Cao and P. B. Messersmith, *Biomater. Sci.*, 2018, **6**, 2487–2495.
- 120 E. Montanari, A. Gennari, M. Pelliccia, C. Gourmel, E. Lallana, P. Matricardi, A. J. McBain and N. Tirelli, *Macromol. Biosci.*, 2016, **16**, 1815–1823.
- 121 O. Mitsunobu, M. Yamada and T. Mukaiyama, *Bull. Chem. Soc. Jpn.*, 1967, **40**, 935–939.
- 122 C. Chen, X. W. Geng, Y. H. Pan, Y. N. Ma, Y. X. Ma, S. Z. Gao and X. J. Huang, *RSC Adv.*, 2020, **10**, 1724–1732.
- 123 J. Wei, G. Wang, F. Chen, M. Bai, Y. Liang, H. T. Wang, D. Y. Zhao and Y. X. Zhao, *Angew. Chem., Int. Ed.*, 2018, **57**, 9838–9843.
- 124 M. M. Zhang, S. X. Zhang, X. X. Liu, H. Chen, Y. F. Ming, Q. Xu and Z. H. Wang, *Environ. Sci. Pollut. Res.*, 2019, **26**, 31834–31845.
- 125 G. Y. Chen, Y. R. Cao, L. Ke, X. X. Ye, X. Huang and B. Shi, *Ind. Eng. Chem. Res.*, 2018, **57**, 16442–16450.
- 126 D. L. Tao, L. Z. Feng, Y. Chao, C. Liang, X. J. Song, H. C. Wang, K. Yang and Z. Liu, *Adv. Funct. Mater.*, 2018, **28**, 1804901.
- 127 N. Sahiner and S. B. Sengel, *Colloids Surf., A*, 2016, **508**, 30–38.
- 128 J. S. Guo, X. G. Tian, D. H. Xie, K. Rahn, E. Gerhard, M. L. Kuzma, D. F. Zhou, C. Dong, X. C. Bai, Z. H. Lu and J. Yang, *Adv. Funct. Mater.*, 2020, **30**, 2002438.
- 129 A. Fujimoto and T. J. Masuda, *J. Agric. Food Chem.*, 2012, **60**, 5142–5151.
- 130 L. Zhang, L. B. Cheng, L. J. Jiang, Y. S. Wang, G. X. Yang and G. Y. He, *J. Sci. Food Agric.*, 2010, **90**, 2462–2468.
- 131 C. Chen, X. Yang, S. J. Li, C. Zhang, Y. N. Ma, Y. X. Ma, P. Gao, S. Z. Gao and X. J. Huang, *Green Chem.*, 2021, **23**, 1794–1804.
- 132 J. A. Stella, A. D'Amore, W. R. Wagner and M. S. Sacks, *Acta Biomater.*, 2010, **6**, 2365–2381.
- 133 A. R. Amini, C. T. Laurencin and S. P. Nukavarapu, *CRC Crit. Rev. Bioeng.*, 2012, **40**, 363–408.
- 134 A. M. Poblath, S. Checa, H. Razi, A. Petersen, J. C. Weaver, K. Schmidt-Bleek, M. Windolf, A. Á. Tatai, C. P. Roth, K. D. Schaser, G. N. Duda and P. Schwabe, *Sci. Transl. Med.*, 2018, **10**, eaam8828.
- 135 J. Gleeson, N. Plunkett and F. O'Brien, *Eur. Cells Mater.*, 2010, **20**, 218–230.
- 136 D. Gan, W. Xing, L. Jiang, J. Fang, C. Zhao, F. Ren, L. Fang, K. Wang and X. Lu, *Nat. Commun.*, 2019, **10**, 1487.
- 137 S. M. Bai, X. L. Zhang, P. Q. Cai, X. W. Huang, Y. Q. Huang, R. Liu, M. Y. Zhang, J. B. Song, X. D. Chen and H. B. Yang, *Nanoscale Horiz.*, 2019, **4**, 1333–1341.
- 138 J. U. Lee and G. H. Kim, *ACS Biomater. Sci. Eng.*, 2018, **4**, 278–289.
- 139 S. M. Bai, X. L. Zhang, X. L. Lv, M. Y. Zhang, X. W. Huang, Y. Shi, C. H. Lu, J. B. Song and H. B. Yang, *Adv. Funct. Mater.*, 2019, **30**, 1908381.
- 140 S. R. Abulatefeh and M. O. Taha, *J. Microencapsulation*, 2015, **32**, 96–105.



- 141 W. Zhang, C. Ling, H. Y. Liu, A. N. Zhang, L. Mao, J. Wang, J. Chao, L. J. Backman, Q. Q. Yao and J. L. Chen, *Chem. Eng. J.*, 2020, **396**, 125232.
- 142 L. Q. Xu, K. G. Neoh and E. T. Kang, *Prog. Polym. Sci.*, 2018, **87**, 165–196.
- 143 W. W. Shen, Q. W. Wang, Y. Shen, X. Gao, L. Li, Y. Yan, H. Wang and Y. Y. Cheng, *ACS Cent. Sci.*, 2018, **4**, 1326–1333.
- 144 H. L. Fan, J. H. Wang and Z. X. Jin, *Macromolecules*, 2018, **51**, 1696–1705.
- 145 C. Y. Shao, M. Wang, L. Meng, H. L. Chang, B. Wang, F. Xu, J. Yang and P. B. Wan, *Chem. Mater.*, 2018, **30**, 3110–3121.
- 146 X. M. Fan, S. B. Wang, Y. Fang, P. Y. Li, W. K. Zhou, Z. C. Wang, M. F. Chen and H. Q. Liu, *Mater. Sci. Eng., C*, 2020, **109**, 110649.
- 147 R. Wang, X. X. Wang, Y. J. Zhan, Z. Xu, Z. Q. Xu, X. H. Feng, S. Li and H. Xu, *ACS Appl. Mater. Interfaces*, 2019, **11**, 37502–37512.
- 148 E. C. Davidson, *Surg., Gynecol. Obstet.*, 1925, **41**, 202–221.
- 149 M. Farokhi, F. Mottaghiab, Y. Fatahi, A. Khademhosseini and D. L. Kaplan, *Trends Biotechnol.*, 2018, **36**, 907–922.
- 150 N. Kojic, M. J. Panzer, G. G. Leisk, W. K. Raja, M. Kojic and D. L. Kaplan, *Soft Matter*, 2012, **8**, 6897–6905.
- 151 M. Parani, G. Lokhande, A. Singh and A. K. Gaharwar, *ACS Appl. Mater. Interfaces*, 2016, **8**, 10049–10069.
- 152 Y. Y. Zheng, Y. Q. Liang, D. P. Zhang, X. Y. Sun, L. Liang, J. Li and Y. N. Liu, *ACS Omega*, 2018, **3**, 4766–4775.
- 153 F. F. Sun, Y. Z. Bu, Y. R. Chen, F. Yang, J. K. Yu and D. C. Wu, *ACS Appl. Mater. Interfaces*, 2020, **12**, 9132–9140.
- 154 M. S. Ma, Y. L. Zhong and X. L. Jiang, *Carbohydr. Polym.*, 2020, **236**, 116096.
- 155 J. Jing, S. F. Liang, Y. F. Yan, X. Tian and X. M. Li, *ACS Biomater. Sci. Eng.*, 2019, **5**, 4601–4611.
- 156 Y. L. Yu, P. F. Li, C. L. Zhu, N. Ning, S. Y. Zhang and G. J. Vancso, *Adv. Funct. Mater.*, 2019, **29**, 1904402.
- 157 M. R. Humphreys, E. P. Castle, P. E. Andrews, M. T. Gettman and M. H. Ereth, *Am. J. Surg.*, 2008, **195**, 99–103.
- 158 N. Li, X. Yang, W. Liu, G. H. Xi, M. S. Wang, B. Liang, Z. P. Ma, Y. K. Feng, H. Chen and C. C. Shi, *Macromol. Biosci.*, 2018, **18**, 1800209.
- 159 C. Chen, W. Sun, X. Wang, Y. Wang and P. Wang, *Int. J. Biol. Macromol.*, 2018, **111**, 1106–1115.
- 160 S. D. Li and L. Huang, *Mol. Pharmaceutics*, 2008, **5**, 496–504.
- 161 H. Yang, Q. Wang, Z. F. Li, F. Y. Li, D. Wu, M. Fan, A. B. Zheng, B. Huang, L. Gan, Y. L. Zhao and X. L. Yang, *Nano Lett.*, 2018, **18**, 7909–7918.
- 162 H. Yang, Q. Wang, W. Chen, Y. B. Zhao, T. Y. Yong, L. Gan, H. B. Xu and X. L. Yang, *Mol. Pharmaceutics*, 2015, **12**, 1636–1647.
- 163 Q. H. Sun, Z. X. Zhou, N. S. Qiu and Y. Q. Shen, *Adv. Mater.*, 2017, **29**, 1606628.
- 164 C. Y. Sun, Y. Liu, J. Z. Du, Z. T. Cao, C. F. Xu and J. Wang, *Angew. Chem., Int. Ed.*, 2016, **55**, 1010–1014.
- 165 Q. Zhou, S. Q. Shao, J. Q. Wang, C. H. Xu, J. J. Xiang, Y. Piao, Z. X. Zhou, Q. S. Yu, J. B. Tang, X. R. Liu, Z. H. Gan, R. Mo, Z. Gu and Y. Q. Shen, *Nat. Nanotechnol.*, 2019, **14**, 799–809.
- 166 H. Xiong, Z. H. Wang, C. Wang and J. Yao, *Nano Lett.*, 2020, **20**, 1781–1790.
- 167 C. Chen, T. H. Ma, W. Tang, X. L. Wang, Y. B. Wang, J. F. Zhuang, Y. C. Zhu and P. Wang, *Nanoscale Horiz.*, 2020, **5**, 986–998.
- 168 H. M. Zhu, G. D. Cao, Y. K. Fu, C. Fang, Q. Chu, X. Li, Y. L. Wu and G. R. Han, *Nano Res.*, 2021, **14**, 222–231.
- 169 J. Liu, Y. Deng, D. Fu, Y. Yuan, Q. L. Li, L. Shi, G. B. Wang, Z. Wang and L. Wang, *Bioact. Mater.*, 2021, **6**, 273–284.
- 170 Y. Wang, Z. Wang, C. Xu, H. Tian and X. Chen, *Biomaterials*, 2019, **197**, 284–293.
- 171 T. Liu, M. K. Zhang, W. L. Liu, X. Zeng, X. L. Song, X. Q. Yang, X. Z. Zhang and J. Feng, *ACS Nano*, 2018, **12**, 3917–3927.
- 172 A. Vargas Jentzsch, A. Hennig, J. Mareda and S. Matile, *Acc. Chem. Res.*, 2013, **46**, 2791–2800.
- 173 J. Li, X. Li, S. Gong, C. Zhang, C. Qian, H. Qiao and M. Sun, *Nano Lett.*, 2020, **20**, 4842–4849.
- 174 Y. B. Wang, F. Liu, N. Yan, S. Sheng, C. N. Xu, H. Y. Tian and X. S. Chen, *ACS Biomater. Sci. Eng.*, 2019, **5**, 4700–4707.
- 175 F. He, M. C. Han, J. Zhang, Z. X. Wang, X. C. Wu, Y. Y. Zhou, L. F. Jiang, S. Q. Peng and Y. X. Li, *Nano Energy*, 2020, **71**, 104650.
- 176 Z. X. Wang, X. C. Wu, J. M. Dong, X. H. Yang, F. He, S. Q. Peng and Y. X. Li, *Chem. Eng. J.*, 2022, **427**, 130905.
- 177 Q. Shi, K. Wu, X. Y. Huang, R. Xu, W. Zhang, J. Bai, S. Y. Du and N. Han, *Colloids Surf., A*, 2021, **618**, 126475.
- 178 T. Chen, R. T. Huang, J. W. Liang, B. Zhou, X. L. Guo, X. C. Shen and B. P. Jiang, *Chem.–Eur. J.*, 2020, **26**, 15159–15169.
- 179 X. Huang, J. Z. Liu, P. Zhou, G. H. Su, T. Zhou, X. X. Zhang and C. H. Zhan, *Small*, 2021, 2104048, DOI: 10.1002/smll.202104048.
- 180 Y. Y. Wang, X. Huang and X. X. Zhang, *Nat. Commun.*, 2021, **12**, 1291.

